Spatial Trends and Historical Deposition of Mercury in Eastern and Northern Canada Inferred from Lake Sediment Cores

D.C.G. MUIR,*,† X. WANG,† F. YANG,† N. NGUYEN,† T. A. JACKSON,† M. S. EVANS,‡ M. DOUGLAS,§ G. KÖCK,|| S. LAMOUREUX,⊥ R. PIENITZ,# J. P. SMOL,▽ W. F. VINCENT,# AND A. DASTOOR○

Environment Canada, Aquatic Ecosystem Protection Research Division, Burlington ON L7R 4A6, Environment Canada, Aquatic Ecosystem Protection Research Division, SaskatoonSK S7N 3H5, Canadian Circumpolar Institute, University of Alberta, Edmonton, AB T6G 2R3, Austrian Academy of Sciences, Dr. Ignaz Seipel-Platz 2, A-1010 Vienna, Austria, Department of Geography, Queen's University, Kingston ON K7L 3N6, Centre d'Etudes Nordiques, Université Laval, Québec Qc G1 V 0A6, Department of Biology, Queen's University, Kingston ON K7L 3N6, and Environment Canada, Air Quality Research Division, Dorval QC H9P 1J3

Received December 14, 2008. Revised manuscript received April 11, 2009. Accepted May 5, 2009.

Recent and historical deposition of mercury (Hg) was examined over a broad geographic area from southwestern Northwest Territories to Labrador and from the U.S. Northeast to northern Ellesmere Island using dated sediment cores from 50 lakes (18 in midlatitudes (41−50°N), 14 subarctic (51−64°N) and 18 in the Arctic (65−83°N)). Distinct increases of Hg over time were observed in 76% of Arctic, 86% of subarctic and 100% of midlatitude cores. Subsurface maxima in Hg depositional fluxes (μg m^{-2} y^{-1}) were observed in only 28% of midlatitude lakes and 18% of arctic lakes, indicating little recent reduction of inputs. Anthropogenic Hg fluxes adjusted for sediment focusing and changes in sedimentation rates ($\Delta F_{adj,F}$) ranged from −22.9 to 61 μg m^{-2} y^{-1} and were negatively correlated ($r = -0.57$, $P < 0.001$) with latitude. Hg flux ratios (FRs; post-1990)/pre-1850) ranged from 0.5 to 7.7. The latitudinal trend for Hg $\Delta F_{adj,F}$ values showed excellent agreement with predictions of the global mercury model, GRAHM for the geographic location of each lake ($r = 0.933$, $P < 0.001$). The results are consistent with a scenario of slow atmospheric oxidation of mercury, and slow deposition of reactive mercury emissions, declining with increasing latitude away from emission sources in the midlatitudes, and support the view that there are significant anthropogenic Hg inputs in the Arctic.

Introduction

Elevated mercury (Hg) in fish has been well documented in midlatitude North American lakes (*1, 2*), and Hg has emerged as a priority contaminant in lakes and rivers of Arctic and subarctic North America (*3*). Hg concentrations in fish are ultimately linked to bioaccumulation of methyl Hg in lakes and their catchments (*4*). Recent studies using Hg isotopes have shown that methyl Hg concentrations in fish responded rapidly to changes in (inorganic) Hg deposition in a lake in the Experimental Lakes Area in northwestern Ontario with the increase coming almost entirely from deposition to the lake surface (*5*). Hg deposition has been modeled using atmospheric transport and deposition models (*6, 7*) which predict significant anthropogenic Hg deposition in Arctic and subarctic regions although declining with increasing north latitude. Yet, there is only limited validation of model predictions because routine Hg wet deposition measurements are limited to south of about 50°N (*8*).

Lake sediments have been shown to be reliable archives for estimating historical Hg accumulation (*9, 10*) although it has been noted that sediments are not especially responsive to changes in Hg deposition over the past 10−20 years owing to slow Hg transport through catchment soils (*11*). Lake sediments have been used to estimate current and historical Hg deposition in numerous midlatitude lakes in North America (*12*−*16*). Recent studies by Mills et al. (*16*) on lakes in south-central Ontario lakes and by Engstrom et al. (*15*) on Minnesota lakes provide anthropogenic Hg enrichment and deposition data for over 200 midlatitude (44−48 °N) lakes. Reviews of Hg deposition to Arctic and subarctic lakes based on sediment cores of early to late-1990s data noted that there was a lack of information on Hg deposition in the eastern Arctic and northern Québec, where no cores from lakes north of 55°N latitude had been analyzed (*17, 18*). Recently Fitzgerald et al. (*19*) studied Hg deposition in five lakes in the north slope of Alaska, and Outridge et al. (*20, 21*) reported on historical sedimentary profiles of Hg in two lakes in the central Canadian Arctic archipelago. Overall, however, little information is available on deposition of Hg to subarctic and Arctic lakes in North America compared to midlatitude regions. Thus while knowledge of Hg deposition in lake sediment cores over large spatial scales could aid understanding of spatial and temporal trends of Hg in fish, the current geographical coverage is poor.

Our objectives were to quantify latitudinal and longitudinal trends of anthropogenic Hg deposition in eastern and northern North America, to investigate variations in Hg deposition, to examine relationships with lake area, catchment/lake area ratio and sedimentation rates, and to compare our results with model predictions.

Materials and Methods

Study Design and Site Selection. Sediment cores were obtained during the period 1998−2005 from lakes in the Canadian Arctic archipelago, subarctic lakes in the southwestern Northwest Territories, Manitoba, Ontario, Québec, and Labrador, and midlatitude lakes in Ontario, Québec, and northeastern U.S. (Figure 1). Full details on the lake characteristics are provided in Supporting Information (SI) Table S1. Lakes were assigned to Arctic (>65°N and above the treeline), subarctic (Labrador, Northern Québec, Ontario

* Corresponding author phone: 905-319-6921; fax: 905-336-6430; e-mail: derek.muir@ec.gc.ca.
† Environment Canada, Aquatic Ecosystem Protection Research Division.
‡ Environment Canada, Aquatic Ecosystem Protection Research Division.
§ University of Alberta.
|| Austrian Academy of Sciences.
⊥ Department of Geography, Queen's University.
Université Laval.
▽ Department of Biology, Queen's University.
○ Environment Canada, Air Quality Research Division.

10.1021/es8035412 CCC: $40.75
Published on Web 05/27/2009

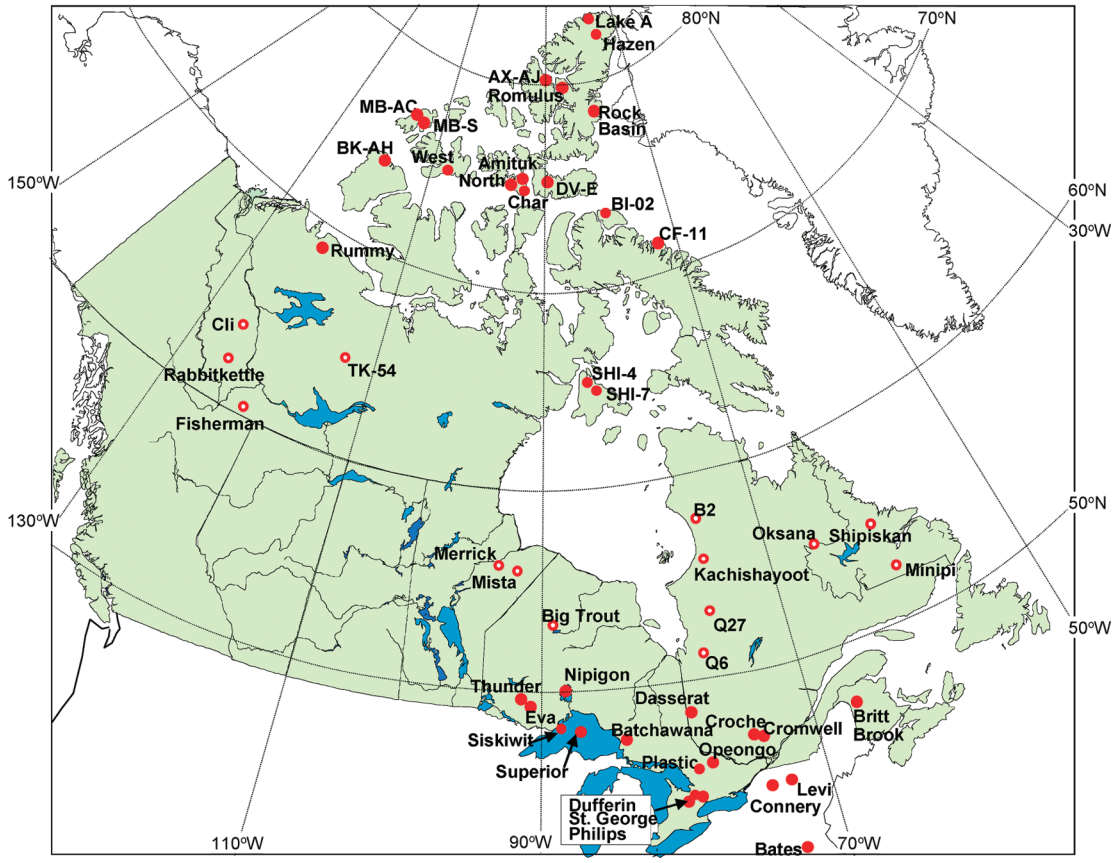

FIGURE 1. Location of the 50 study lakes. Midlatitude lakes were south of 51°N, subarctic lakes (open symbols) from 51−65°N and Arctic lakes north of 65°N. See SI Table S1 for additional information on each lake.

TABLE 1. Pearson Correlation Coefficients[a] for Correlations of Lake Characteristics with Latitude and Longitude

	N	latitude	long-itude	precip[b] (mm)	% organic carbon	log A_L	log A_C	A_C/A_L	focusing factor[c]	Al flux ratio[d]
precipitation (mm)	50	−0.941**	−0.519**							
% organic carbon	47	−0.421*	−0.278	0.424*						
Log A_L	50	−0.224	−0.077	0.166	−0.150					
Log A_C	50	−0.125	−0.107	0.092	−0.241	0.897**				
A_C/A_L	50	0.138	−0.114	−0.112	−0.191	−0.093	0.241			
focusing factor	49	0.456**	0.120	−0.429**	−0.357*	0.092	0.212	0.444**		
Al flux ratio	48	−0.139	−0.155	0.142	−0.009	−0.056	−0.013	0.014	0.054	
sedimentation rate	49	0.347*	0.172	−0.338*	−0.368*	0.017	0.147	0.356	0.717**	0.185
sedimentation ratio[e]	49	−0.114	−0.116	0.105	−0.007	−0.056	−0.054	−0.004	0.014	0.915**

[a] ** and * = Significant Pearson correlation coefficients at $P = 0.01$ and 0.05, respectively, using uncorrected probabilities. [b] Average (1970−2000) precipitation at nearest Environment Canada (http://www.climate.weatheroffice.ec.gc.ca/climateData/canada_e.html) or NOAA (http://cdo.ncdc.noaa.gov/cgi-bin/climatenormals/climatenormals.pl) station. [c] Focusing factor based on average excess ^{210}Pb divided by known or estimated ^{210}Pb for the latitude of the individual lake. For further details on estimated ^{210}Pb see the Supporting Information. [d] Aluminum (Al) flux = ((recent (post-1990)/pre-1850) were calculated to estimate erosional/aoelian inputs. [e] Sedimentation ratio = CRS estimated sediment flux, g m^{-2} y^{-1} ((recent (post-1990)/pre-1850).

and Manitoba >51°N and Northwest Territories), and midlatitude (south of 51°N) groups.

Sample Collection and Dating. In brief, cores (6−10 cm diam) were obtained from the deepest point in each lake avoiding steep sloped areas. Cores were extruded and sliced into 0.5 or 1 cm sections (SI Table 1). Sediment cores were dated using the ^{210}Pb and/or ^{137}Cs methods, and sedimentation rates and dates were estimated using the constant rate of supply (CRS) model (*22*). Only cores with interpretable ^{210}Pb or ^{137}Cs stratigraphy were selected for analysis; they typically yielded 10−20 post-1800 core sections or horizons, per core. Further details on collection, dating, and analysis are provided in the Supporting Information.

Mercury and Multielement Analysis. Freeze-dried subsamples were placed in Teflon vessels and acid-digested with a mixture of nitric and hydrochloric acids and hydrogen peroxide (ratio 9:2:1) in a high pressure microwave oven. Total Hg was determined by cold vapor atomic absorption spectrometry. A subset of cores were analyzed by direct combustion using a DMA-80 (Milestone Instruments, Shelton, CT). Total Al and Zn were determined by inductively coupled plasma-mass spectrometry (ICP-MS) (PQ-2, VG Elemental) and manganese (Mn) and iron (Fe) using ICP-atomic emission spectrometry (AES). Organic carbon (OC) was determined by CHN analyzer in subsamples from 47 of 50 cores.

Flux Calculations and Statistical Analysis. Recent and preindustrial horizons in each core were defined by the median ages assigned to each core section using the CRS

model. Hg fluxes, flux ratios (FR), and enrichment factors (EFs) were calculated as

Flux (F) (μg m^{-2} y^{-1}) = [dry wt concn] × ^{210}Pb-derived sedimentation rates for each core horizon.

Anthropogenic flux, ΔF (μg m^{-2} y^{-1}) = F_{recent} (post-1990) − F_{preind} (preindustrial; pre-1850), FR = F_{recent}/F_{preind} and EF = recent (post-1990)/preindustrial Hg concentrations.

Fluxes of Al were calculated to investigate inputs of a primarily lithogenic element and Al flux ratios [(recent (post-1990) − pre-1850)/pre-1850] were calculated to estimate erosional and aeolian inputs. After confirming a strong correlation of Al flux ratio and the ratio of ^{210}Pb derived recent and preindustrial sedimentation rates ($r = 0.915$, $P < 0.001$, $N = 34$), Hg fluxes for each horizon were adjusted for sedimentation and an anthropogenic Hg flux ΔF_{adj} was calculated using the equation of Perry et al. (*13*):

$$\Delta F_{adj} = F_{recent} - F_{pre\text{-}ind} - (F_{pre\text{-}ind} \times \text{sedimentation ratio} - F_{pre\text{-}ind}) \quad (1)$$

As noted by Perry et al. (*13*) if the pre-1850 sedimentation rate equals the post-1850 sedimentation rate, the sedimentation ratio = 1 and no adjustment is made. However, in horizons where the sedimentation rate is higher, the ratio adjusts for the dilution effect of increased sedimentation.

Sediment particle focusing factors (FF) were estimated for all cores dated by dividing the observed ^{210}Pb flux (Bq m^{-2}y^{-1}) by the predicted ^{210}Pb flux for the same latitude based on soil ^{210}Pb measurements from 41.5 to 81.5°N latitude (see SI Table S2 and Figure S1 and references therein). Recent fluxes and $\Delta F_{adj,F}$ were adjusted by dividing by FF.

Correlations were performed using Microsoft Excel and Systat 12 (Systat Software Inc. Chicago IL). Lake area (A_L), catchment area (A_C) and Hg fluxes were log transformed to yield normally distributed data (Shapiro−Wilk test; $P > 0.10$).

Modeled Hg Deposition. The global/regional atmospheric heavy metals model (GRAHM) (*6, 23*) was used to predict terrestrial anthropogenic Hg fluxes for each lake location. A description of this model is given by Dastoor and Laroque (*6*) and it was recently modified to include parametrizations for halogen-mediated mercury chemistry, deposition, and re-emission of mercury during spring and summer in the Arctic (*23*). Model simulations were performed for year 2001 at 50 km horizontal resolution using anthropogenic Hg emissions for year 2000 and terrestrial and oceanic emissions as described in Dastoor et al. (*23*). Net deposition of Hg to the surface in the geographic region of each of the 50 lakes was predicted based on their latitude/longitude. In Arctic and subarctic regions the model simulates rapid revolatilization of mercury in addition to the deposition represented by mercury depletion events (MDEs), which are subtracted from the deposition.

Results

Lake Characteristics, Sedimentation Rates, and Elemental Profiles. The lakes ranged widely in surface area (MB-AC = 0.0017 km^2; Superior = 82170 km^2); 37 of 50 were <10 km^2 (SI Table S1). Lake and catchment areas, as well as A_C/A_L were unrelated to lake latitude or longitude (Table 1). Most cores exhibited near-exponential declines in excess^{210}Pb with depth, indicating relatively constant rates of sediment accumulation (see SI Figure S2). Sedimentation rates based on the CRS model ranged from 10 to 1000 g m^{-2} y^{-1} (SI Table S1) and were not significantly correlated with latitude, A_L or A_C (Table 1). Sedimentation rates were generally low and the top 10 cm of most cores included sediments deposited over the past ~150 years. Sedimentation rate was significantly correlated with focusing factor ($r = 0.700$; $P < 0.001$). Sedimentation rates were >10% higher in the period 1990−2000 than in the years 1800−1900 in 27 of 49 lakes; 11 of 49 had 2× higher rates. The increased sedimentation estimated from the ratio of the CRS sedimentation rates in recent and preindustrial horizons, was unrelated to latitude, longitude, average sedimentation rate, or to average annual precipitation for each location (Table 1).

Concentrations of Al, an indicator of geogenic inputs, were available for 35 lakes and showed relatively little variation with deposition year with only 12 lakes having positive correlations and 2 having negative (SI Table S3). Al concentrations within lakes were generally not correlated with sedimentation rate in Arctic and subarctic lakes (SI Table S3). Zn concentrations were correlated with sedimentation rate in <20% of Arctic and subarctic lakes (SI Table S3). However, a slightly higher frequency of positive correlations of both Al and Zn with sedimentation rates was found in midlatitude lakes (22 and 36%, respectively). Overall, sedimentation rate did not appear to have a large lithogenic component, i.e., from erosion or aeolian inputs.

The higher recent sedimentation rates estimated using the CRS model could also be due to the flattening of the slope of the ^{210}Pb activity profile near the sediment surface due to bioturbation or to diagenetic dilution of the ^{210}Pb due to accumulation of Fe oxides at the surface (*19, 24*). Bioturbation is unlikely to be a major factor because almost all these lakes are all cold, oligotrophic systems (*25*), however, no quantitative assessment of density of benthic fauna of each lake was available. As for Fe diagenesis resulting in increased Fe in surface sediments and thus increased dry mass, total Fe concentrations increased with deposition year in 10 of 18 (56%) midlatitude cores but in only 2 of 17 arctic lakes (SI Table S3). Thus Fe diagenesis resulting in increased Fe in surface sediments (and thus increased dry mass in surface horizons) may have played a role in influencing estimated sedimentation rates at least in midlatitude lakes as discussed by Gubala et al. (*24*).

Our results for sedimentation rates in Arctic lakes are in general agreement with several recent studies which have shown higher sedimentation in late 20th century horizons compared to 19th century horizons (*19, 20*). Lindeberg et al. (*26*) concluded that changes in the influx of material from regional aeolian activity resulted in large fluctuations in Hg and Pb concentrations in pre-19th century sediments of Greenland lakes. On the other hand, Lockhart et al. (*27*) did not observe differences in recent and preindustrial sedimentation rates in a series of 16 cores ranging from central midlatitude Canada to Lake Hazen. Mean annual snowfall has increased in the central Canadian archipelago (*28*) suggesting greater snowmelt runoff leading to greater erosional inputs in some catchments. The disappearance of shallow ponds in the islands of the Canadian Arctic archipelago has been attributed to increased evaporation/precipitation ratios (*29*) may be an indication of the more rapid drying of lake catchments which could result in greater aeolian inputs for some lakes.

Percent OC of surface sediments declined weakly with latitude (Table 1) ($r = -0.421$, $P = 0.003$), whereas sediment particle focusing factor increased with latitude ($r = 0.456$, $P = 0.005$). Sediment OC has often been used to normalize Hg results because it is assumed that most catchment related Hg enters lakes associated with organic matter. Indeed % OC was positively correlated with Hg concentrations in 15 of 47 lakes and % OC increased with year of deposition in the same lakes (SI Table S3). Bindler et al. (*30*) also found the % OC also increased over time in the three dated cores from Greenland. Outridge et al. (*20, 21*) reported increasing % OC in Amituk Lake, as well as in lake DV09 on Devon Island, and also noted a strong correlation of Hg concentrations with algal-derived organic matter. We found that % OC was >10% higher in the surface section compared with horizons dated to approximately 1800−1900 in 26 of 47 cores for which we

TABLE 2. Mean Concentrations of Hg in Surface Samples, Percent of Lakes with Subsurface Maxima, Mean Flux Ratios (FR), Recent and Pre-Industrial Fluxes, and Adjusted Anthropogenic Fluxes ($\Delta F_{adj,F}$)

region	N[a]	95% CI	μg/g Hg concn	max subsurface flux[b]	max subsurface concn[b]	FR[c]	Hg F_{recent}[d]	Hg F_{preind}[d]	Hg $\Delta F_{adj,F}$[e]
Arctic	18	mean	0.08	18%	17%	2.16	11.4	6.6	2.8
(65−83°N)		95% CI	0.04			0.53	6.4	3.4	2.0
subarctic	14	mean	0.13	25%	33%	2.50	26.9	14.8	7.5
(51−64°N)		95% CI	0.03			0.75	11.8	9.8	5.9
midlatitude	18	mean	0.24	28%	22%	3.56	63.5	24.9	26.8
(41−50°N)		95% CI	0.08			1.00	16.9	9.9	7.2
overall	50	mean	0.15	24%	24%	2.76	34.5	15.7	12.5
		95% CI	0.04			0.48	9.7	5.1	4.4

[a] Arithmetic mean Hg concentrations (ug/g dry wt) are reported for 50 lakes. Fluxes are reported 49 lakes − individual results are presented in SI Table S4. [b] Percent showing maximum concentrations or fluxes in subsurface horizons based on two consecutive near surface samples having >10% lower concentrations or fluxes. [c] FR = flux ratio = F_{recent}/F_{preind}. [d] Recent and preindustrial fluxes (μg m^{-2} y^{-1}) corrected for particle focusing. [e] Adjusted anthropogenic flux (μg m^{-2} y^{-1}) = $\Delta F_{adj,F}$ = (recent flux-preindustrial flux − (preindustrial flux × SR − preindustrial flux))/FF where SR = recent to preindustrial sedimentation ratio. See eq 1.

TABLE 3. Results of Simple Correlations of $\Delta F_{adj,F}$, F_{recent}, and $F_{pre\text{-}ind}$, and Flux Ratios (FR) of Mercury with Various Lake Characteristics[a]

correlation	comparison	*r*	P	N
with latitude/longitude	$\Delta F_{adj,F}$ vs latitude	**−0.572**	**<0.001**	49
	F_{recent}[b] vs latitude	**−0.684**	**<0.001**	49
	F_{preind}[b] vs latitude	**−0.501**	0.001	49
	FR vs latitude	**−0.295**	0.040	49
	FR vs longitude	−0.261	0.070	49
with % organic carbon[c]	$\Delta F_{adj,F}$ vs sediment % OC	0.195	0.189	46
	F_{recent} vs % OC	**0.301**	**0.040**	46
	F_{preind} vs % OC	**0.324**	**0.027**	46
with lake properties (all lakes)	$\Delta F_{adj,F}$ vs log A_L	0.000	0.998	49
	$\Delta F_{adj,F}$ vs A_C/A_L	−0.010	0.945	49
with midlatitude lake catchment area[d]	F_{recent} vs A_C	**−0.569**	0.013	18
	F_{preind} vs A_C	**−0.562**	0.015	18

[a] $\Delta F_{adj,F}$, recent, and preindustrial fluxes were log transformed for all correlations. Statistically significant relationships are bolded. [b] Recent and preindustrial fluxes (μg m^{-2} y^{-1}) corrected for particle focusing. [c] %OC = % organic carbon of recent (post 1990) horizons. [d] For midlatitude lakes only.

had OC profiles while only 3 of 47 showed a >10% decrease. The increased %OC could be due to progressive loss of carbon following burial as shown by Gälman et al. (*31*) for a varved lake sediment in northern Sweden. Alternatively, increased autochthonus production could be occurring, particularly in Arctic lakes (*19, 20*). Given that % OC was significantly correlated with latitude while the sedimentation ratio was not (Table 1), we concluded that adjustment of fluxes using the sedimentation ratio (eq 1) was more appropriate than % OC since the latter might introduce a bias for evaluating latitudinal trends.

Recent and Preindustrial Hg Fluxes. Anthropogenic mercury flux, $\Delta F_{adj,F}$, ranged from −22.9 to 61 μg m^{-2} y^{-1} averaging 2.8, 7.5, and 26.8 μg m^{-2} y^{-1} in Arctic, subarctic, and midlatitude lakes, respectively (Table 2). Hg $\Delta F_{adj,F}$ had a significant negative correlation with latitude ($r = -0.572$; $P = <0.001$) (Table 3), but was not correlated with lake area, A_C/A_L or % OC in sediment. The lowest value $\Delta F_{adj,F}$ was for Rabbitkettle Lake in southwestern NWT (SI Table S4). Omitting this lake, which had higher Hg fluxes than other subarctic lakes despite its remote location, improved the correlation with latitude (Figure 2A, $r = -0.670$; $P < 0.001$).

The net anthropogenic Hg deposition fluxes simulated by GRAHM for the region of each lake declined significantly with latitude (Figure 2B, $r = 0.933$, $P < 0.001$). Individual predicted values are given in SI Table S4. These predicted values represent the average deposition within the model grid cell for a single year (2001).

Hg F_{recent} (corrected for particle focusing but not for sedimentation) also showed significant negative correlation with latitude ($r = -0.684$; $P < 0.001$; Table 3 and Figure 2C) and focus corrected preindustrial fluxes (F_{preind}) were also correlated ($r = -0.501$, $P = 0.001$; Table 3 and Figure 2D). Uncorrected recent fluxes were also significantly correlated with latitude while preindustrial fluxes showed no correlation (SI Figure S3). Results for individual lakes are provided in SI Table S4. F_{recent} and F_{preind} Hg were weakly correlated with % OC ($P = 0.040$ and 0.027, respectively) but not with longitude (data not shown). F_{recent} and F_{preind} were also correlated with precipitation ($P < 0.001$); however, precipitation and latitude were highly correlated (Table 1).

Recent Hg fluxes in midlatitude lakes have been shown to be correlated with A_C/A_Lwhile preindustrial fluxes were generally not correlated (*12, 32−34*). In this study F_{recent} and F_{preind} for Hg were not correlated with A_C/A_L, A_L, or A_C, when all lakes were combined (Table 3). However, in midlatitude lakes F_{recent} and F_{preind} for Hg were negatively correlated with A_C ($P = 0.013$ and 0.015, respectively; $N = 18$) (Table 3) (SI Figure S4). Grigal (*35*) noted that the flux of Hg via catchment streamflow showed a clear tendency for lower annual flux with increasing watershed size. Our results are thus in general agreement with the earlier studies and they

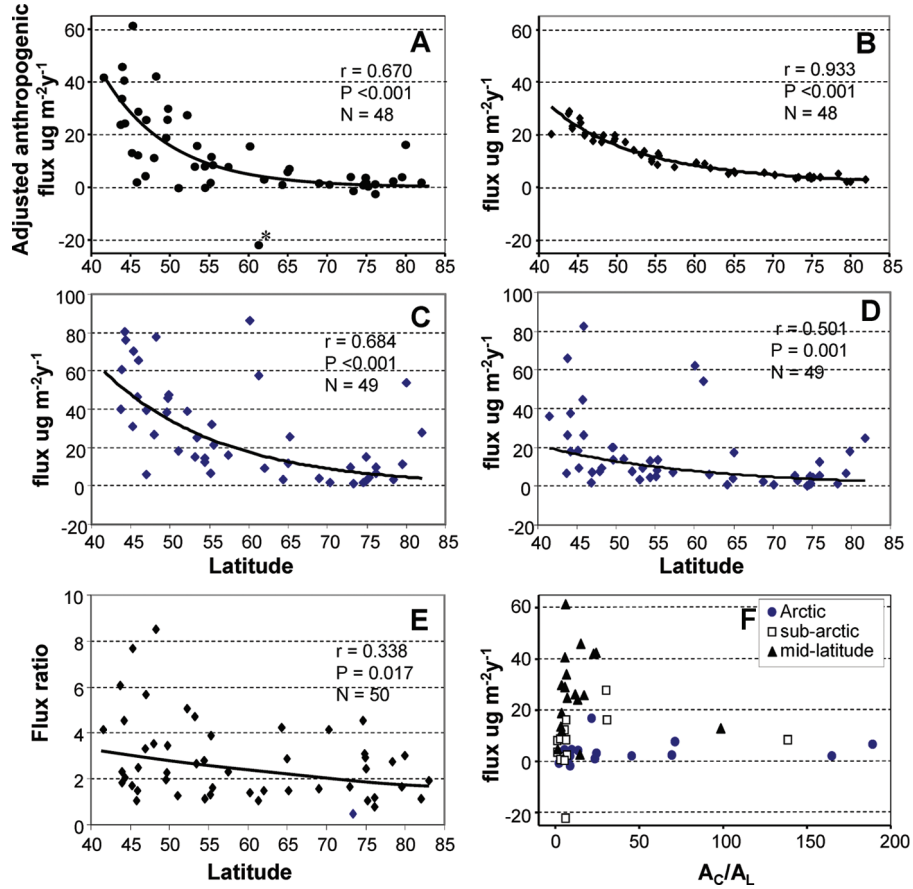

FIGURE 2. (A) Relationship of adjusted anthropogenic flux $\Delta F_{adj,F}$ for mercury vs latitude in dated sediment cores from midlatitude, subarctic and Arctic lakes, (B) comparison with net flux predicted for each lake location using GRAHM, (C) focus corrected recent fluxes, (D) focus corrected preindustrial fluxes, (E) the latitudinal trend of mercury flux ratios. All statistics for flux vs latitude are based on log transformed flux data. A single data point in A marked with a * was omitted to calculate the correlation coefficients. No significant trends of $\Delta F_{adj,F}$ with catchment to lake area ratio (A_C/A_L) were found (F).

underline the importance of catchment inputs for Hg transport, with increasing in importance in larger forested catchments common to all of the midlatitude lakes. The lack of correlation with A_C/A_L may be a consequence of large range of A_C/A_L (0.6−189) due to a more diverse group of lakes compared to other studies. Above A_C/A_L values of about 30, $\Delta F_{adj,F}$ values appear to be relatively constant and not related to geographic location (Figure 2F).

Hg FRs ranged from 0.5 to 7.7, averaging 2.76 (SI Table S4). FRs were very weakly correlated with latitude ($P = 0.04$ and 0.03) (Figure 2E). The FRs were not significantly correlated with longitude ($P = 0.070$), nor with % OC, A_C/A_L, or A_L (data not shown).

Historical Profiles of Hg. There was a general increase of Hg concentrations with deposition year in almost all cores and significant ($P < 0.05$) positive correlations of Hg concentration and year in 76% of Arctic, 86% of subarctic, and 100% of midlatitude lakes (SI Table S3). However, 18% of arctic lakes, 33% of subarctic lakes, and 22% of midlatitude lakes had subsurface maxima for Hg concentrations and 18, 25, and 28%, respectively, when based on flux (Table 2). Plots of Hg concentrations and fluxes versus CRS dates for individual sediment cores are shown in SI Figure S5.

Overall historical trends in focus and sedimentation corrected anthropogenic Hg deposition rates (i.e., $\Delta F_{adj,F}$ for each sediment horizon analyzed) in Arctic, subarctic and midlatitude lakes are presented in Figure 3. The curves were generated by calculating the average flux for 20 year time intervals from 1840 to 1900, 10 year time intervals from 1901 to 1990, and 5 year intervals from 1991 to 2005. Results for individual lakes are provided in SI Figure S6. Generally

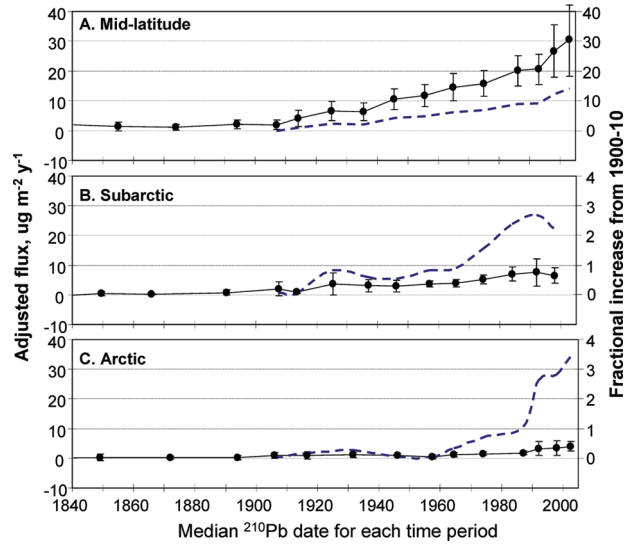

FIGURE 3. Average (±95% confidence limits) historical profiles of anthropogenic mercury deposition fluxes ($\Delta F_{adj,F}$, $\mu g\ m^{-2}\ y^{-1}$) in midlatitude, subarctic, and Arctic sediment cores for all Arctic, subarctic, and midlatitude lakes over 5−20 year time intervals. Dashed line shows the fractional increase of $\Delta F_{adj,F}$ over the same time intervals relative to values for 1900−1910. Individual lake results are given in SI Figure S5.

$\Delta F_{adj,F}$ showed a distinct increase in post-1900 horizons in midlatitude cores, post-1920−1940 in subarctic cores and post-1950 in Arctic cores. The fractional increase of $\Delta F_{adj,F}$

relative to the anthropogenic flux in 1900−1910, shown by the dashed line in Figure 3, shows a 14.5-fold increase during the 20th century in midlatitude lakes, a 2.7-fold in subarctic, and 3.5 fold in the Arctic lakes. There is a proportionally small anthropogenic enhancement in Arctic and subarctic lakes compared to midlatitude lakes owing to relatively high background (preindustrial) Hg fluxes across all latitudes (Figure 2D; SI Figure S3).

Comparison with Other Studies of Hg Flux Ratios and Adjusted Fluxes. The range of FR values for Hg observed in this study is similar to previous reports for FRs and enrichment factors (EFs; Hg $\text{concn}_{\text{recent}}$/Hg $\text{concn}_{\text{preind}}$) in Arctic and north temperate lakes in Canada and Alaska (*17, 36*) but lower than found in the northeastern U.S. (*12*). Hg EFs for 202 lakes in south-central Ontario ranged from 0.5 to 5.1. Hg EFs for 21 lakes in West Greenland averaged 2.9 (range 0.8−11.2) (*30*), which overall, is higher than the FRs in the present study.

The Hg fluxes in North America reported by Landers et al. (*17*), based on recent horizons of cores collected in the 1980s and early 1990s over a similar range of latitude as this study, ranged from about 3 to 52 $\mu g\ m^{-2}\ y^{-1}$, whereas preindustrial fluxes ranged from 2.5 to 54 $\mu g\ m^{-2}\ y^{-1}$. These fluxes are within the range observed in this study (focus corrected). Perry et al. (*13*) reported corrected recent Hg deposition rates ($\Delta F_{adj,F}$) of 10−60 $\mu g\ m^{-2}\ y^{-1}$, averaging 25 $\mu g\ m^{-2}\ y^{-1}$ for 29 lakes in the northeastern U.S., with maximum values generally being reached between 1970 and 1990. We used the same adjustment and our average $\Delta F_{adj,F}$ for midlatitude lakes (26.8 $\mu g\ m^{-2}\ y^{-1}$) agrees well with the latter study. Two study lakes, Levi (VT) and Bates (CT) had $\Delta F_{adj,F}$ of 41 and 45 $\mu g\ m^{-2}\ y^{-1}$, respectively, similar to other lakes in that region (*13*).

Lockhart et al. (*27*) studied a series of lakes along a north−south transect and reported greatest anthropogenic enrichments in Hg occurred in central/southern Canada with a 2 fold increase over the past half century. Their fluxes for Lakes Amituk (3.9 $\mu g\ m^{-2}\ y^{-1}$) and Hazen (23 $\mu g\ m^{-2}\ y^{-1}$) were in good agreement with the present study (SI Table S4). Two more recent studies of Arctic lakes also found Hg fluxes within the range reported in this study. Bindler et al. (*30*) found recent fluxes of Hg in dated cores from three west Greenland lakes ranging from about 5 to 10 $\mu g\ m^{-2}\ y^{-1}$, and Fitzgerald et al. (*19*) estimated whole lake Hg fluxes of approximately 2.5−5.0 $\mu g\ m^{-2}\ y^{-1}$ for five lakes in northern Alaska after correcting for soil erosion.

Comparison with Predicted Trends in Fluxes for Hg. Reduction in overall atmospheric Hg emissions in North America and Europe of about 10 and 50%, respectively, between 1990 and 2000 have been reported, whereas Asian sources (mainly China) increased by 40% over the same time period (*37*). Thus, midlatitude North American lakes might be expected to show declining Hg deposition, and there is evidence of declining Hg fluxes in some studies (*13, 27, 38*). However, other recent studies of remote midlatitude lakes show limited or no decline (*15, 16*) which agrees with our observations for 72% of the 18 midlatitude lakes in this study and with the average decadal trends (Figure 3). The absence of a relatively sharp downturn reflects the slow response of lake sediments that has been attributed to the strong retention of Hg within watershed soils and biomass (*5, 13*).

Independent evidence for whether Hg deposition is increasing or decreasing in Arctic lakes is very limited. The Canadian Arctic archipelago, where almost all our high latitude study lakes were located, is very remote, and north of about 70° latitude, is influenced mainly by Asian and European atmospheric sources (*39, 40*). Analysis of time series for gaseous elemental Hg (GEM) concentrations over the period of 1995−2005 have shown no evidence of a decline at Alert on northern Ellesmere Island (*41*). Boutron et al. (*42*) reported a 40 year record of Hg in snow cores from the Greenland icecap which showed relatively constant concentrations in the 1980s, unlike increases observed in sediment cores in Greenland over the same period (*30*). Fitzgerald et al. (*19*) concluded that there was significant anthropogenic Hg deposition to lakes in the Toolik Lake area of northern Alaska due to a combination of inputs from polar sunrise MDEs and reactive gaseous Hg dry deposition. Using a relationship between Hg concentrations in precipitation and ^{210}Pb activity from remote northern hemispheric locations they estimated a Hg flux for northern Alaska of 2.2 ug $m^{-2}\ yr^{-1}$ which is similar to the average $\Delta F_{adj,F}$ of 2.8 $\mu g\ m^{-2}\ yr^{-1}$ for 18 Arctic lakes in this study. Brooks et al. (*43*) estimated net gains of Hg of 0.7 ± 0.2 $\mu g\ m^{-2}$ at Barrow, AK as a result of spring time MDEs.

The GRAHM predicted average (±SD) Hg fluxes of 4.1 ± 1.1, 11 ± 3.1, and 22 ± 3.9 $\mu g\ m^{-2}\ y^{-1}$ for the Arctic, subarctic, and midlatitude lake locations, respectively. This was in very good agreement with the general trend seen for $\Delta F_{adj,F}$ in Figure 2A and the average fluxes for each region (Table 2). Other Hg deposition model estimates for eastern and northern North America also predict declining fluxes with latitude (*6−8, 44, 45*). The Danish Eulerian Hemispheric model (DEHM) predicts annual Hg deposition with Hg depletion events ranging from >18 $\mu g\ m^{-2}\ y^{-1}$ in eastern North America to 6−12 $\mu g\ m^{-2}\ y^{-1}$ in the Canadian Arctic archipelago (*7*). Miller et al. (*8*) estimated (dry + wet) Hg deposition for rural areas of the northeastern U.S. and adjacent Canadian provinces ranging from about 4 to 30 $\mu g\ m^{-2}\ y^{-1}$ which is good agreement with Hg $\Delta F a_{dj,F}$'s calculated from sediment deposition for this region. Further discussion of model results is given in the Supporting Information.

The agreement between modeled and measured deposition lends additional support to the hypothesis that most Hg deposited from MDEs is revolatilized (*46*). Whereas most of the Hg deposition is predicted to occur over the ocean near sources of Br and BrO (*23*) near shore terrestrial environments could nevertheless receive greater deposition (*46−48*). We examined this question for the 18 Arctic and 2 subarctic lakes in this study that were within 80 km of the ocean. No significant trend was found between Hg FR or with $\Delta F_{adj,F}$ and log distances or square root of the distance, even after omitting the most distant lake (SI Figure S7), suggesting little net effect. To our knowledge this is the most geographically extensive study of Hg fluxes to lake sediments in North America. While a declining trend away from midlatitude emission sources was observed, subarctic and Arctic lakes nevertheless had significant anthropogenic inputs. These observations are consistent with "Hypothesis 2" discussed by Lindberg et al. (*11*) of slow atmospheric oxidation of mercury, slow deposition of reactive mercury emissions, and increasing importance of global sources in remote regions.

Acknowledgments

Funding for the project was provided by the Northern Ecosystem Initiative of Environment Canada, ArcticNet, the Northern Contaminants Program of Indian and Northern Affairs Canada and the Toxic Substances Research Initiative (Health Canada/Environment Canada, 1999−2002). The many people and agencies who made core collection and analysis possible are thanked in the Supporting Information. The extensive annual logistical support from Polar Continental Shelf Project (Natural Resources Canada) made possible collection in the Canadian archipelago. The paper is dedicated to the memory of Doug Halliwell (Environment Canada, Yellowknife) who collected cores in the NWT and Ven Cheam (Environment Canada, Burlington ON) for initiating the project. Thanks to Laurier Poissant (Environment Canada, Montreal) for helpful comments on the initial

manuscript and Daniel Figueras (Environment Canada, Dorval) for GRAHM modelling.

Supporting Information Available

Additional explanatory text, four Tables, and seven Figures. This material is available free of charge via the Internet at http://pubs.acs.org.

Literature Cited

(1) Ontario Ministry of Environment. *Guide to Eating Ontario Sport Fish*, 24th ed.; Ontario Ministry of the Environment: Toronto, ON Canada, 2003.

(2) U.S. Environmental Protection Agency. *National Listing of Fish Advisories*, EPA-823-F-05-004; U.S. Environmental Protection Agency, Office of Water: Washington, DC, 2004; p 6.

(3) Lockhart, W. L.; Stern, G. A.; Low, G.; Hendzel, M.; Boila, G.; Roach, P.; Evans, M. S.; Billeck, B. N.; DeLaronde, J.; Friesen, S.; Kidd, K.; Atkins, S.; Muir, D. C. G.; Stoddart, M.; Stephens, G.; Stephenson, S.; Harbicht, S.; Snowshoe, N.; Grey, B.; Thompson, S.; DeGraff, N. A history of total mercury in edible muscle of fish from lakes in northern Canada. *Sci. Total Environ.* **2005**, *351*, 427–463.

(4) Munthe, J.; Bodaly, R. A.; Branfireun, B. A.; Driscoll, C. T.; Gilmour, C. C.; Harris, R.; Horvat, M.; Lucotte, M.; Malm, O. Recovery of mercury-contaminated fisheries. *Ambio* **2007**, *36*, 33–44.

(5) Harris, R. C.; Rudd, J. W. M.; Amyot, M.; Babiarz, C. L.; Beaty, K. G.; Blanchfield, P. J.; Bodaly, R. A.; Branfireun, B. A.; Gilmour, C. C.; Graydon, J. A.; Heyes, A.; Hintelmann, H.; Hurley, J. P.; Kelly, C. A.; Krabbenhoft, D. P.; Lindberg, S. E.; Mason, R. P.; Paterson, M. J.; Podemski, C. L.; Robinson, A.; Sandilands, K. A.; Southworthn, G. R.; St. Louis, V. L.; Tate, M. T. Whole-ecosystem study shows rapid fish-mercury response to changes in mercury deposition. *Proc. Nat. Acad. Sci. U. S. A.* **2007**, *104*, 16586–16591.

(6) Dastoor, A. P.; Larocque, Y. Global circulation of atmospheric mercury: A modelling study. *Atmos. Environ.* **2004**, *38*, 147–161.

(7) Christensen, J. H.; Brandt, J.; Frohn, L. M.; Skov, H. Modelling of mercury in the Arctic with the Danish Eulerian Hemispheric Model. *Atmos. Chem. Phys.* **2004**, *4*, 2251–2257.

(8) Miller, E. K.; Vanarsdale, A.; Keeler, G. J.; Chalmers, A.; Poissant, L.; Kamman, N. C.; Brulotte, R. Estimation and mapping of wet and dry mercury deposition across northeastern North America. *Ecotoxicology* **2005**, *14*, 53–70.

(9) Biester, H.; Bindler, R.; Martinez-Cortizas, A.; Engstrom, D. R. Modeling the past atmospheric deposition of mercury using natural archives. *Environ. Sci. Technol.* **2007**, *41*, 4852–4860.

(10) Lockhart, W. L.; Macdonald, R. W.; Outridge, P. M.; Wilkinson, P.; DeLaronde, J. B.; Rudd, J. W. M. Tests of the fidelity of lake sediment core records of mercury deposition to known histories of mercury contamination. *Sci. Total Environ.* **2000**, *260*, 171–180.

(11) Lindberg, S.; Bullock, R.; Ebinghaus, R.; Engstrom, D.; Feng, X.; Fitzgerald, W.; Pirrone, N.; Prestbo, E.; Seigneur, C. A synthesis of progress and uncertainties in attributing the sources of mercury in deposition. *Ambio* **2007**, *36*, 19–32.

(12) Kamman, N. C.; Engstrom, D. R. Historical and present fluxes of mercury to Vermont and New Hampshire lakes inferred from 210Pb dated sediment cores. *Atmos. Environ.* **2002**, *36*, 1599–1609.

(13) Perry, E.; Norton, S. A.; Kamman, N. C.; Lorey, P. M.; Driscoll, C. T. Deconstruction of historic mercury accumulation in lake sediments, northeastern United States. *Ecotoxicology* **2005**, *14*, 85–99.

(14) Lamborg, C. H.; Fitzgerald, W. F.; Damman, W. H.; Benoit, J. M.; Balcom, P. H.; Engstrom, D. R. Modern and historic atmospheric mercury fluxes in both hemispheres: global and regional mercury cycling implications. *Global Biogeochem. Cycles* **2002**, *16*, 1104–1115.

(15) Engstrom, D. R.; Balogh, S. J.; Swain, E. B. History of mercury inputs to Minnesota lakes: Influences of watershed disturbance and localized atmospheric deposition. *Limnol. Oceanogr.* **2007**, *52*, 2467–2483.

(16) Mills, R. B.; Paterson, A. M.; Blais, J. M.; Lean, D. R. S.; Smol, J. P.; Mierle, G. Factors influencing the achievement of steady state in mercury contamination among lakes and catchments of south-central Ontario Can. *J. Fish. Aquat. Sci.* **2009**, *66*, 187–200.

(17) Landers, D. H.; Gubala, C.; Verta, M.; Lucotte, M.; Johansson, K.; Vlasova, T.; Lockhart, W. L. Using lake sediment mercury flux ratios to evaluate the regional and continental dimensions of mercury deposition in arctic and boreal ecosystems. *Atmos. Environ.* **1998**, *32*, 919–928.

(18) Braune, B.; Outridge, P.; Wilson, S.; Bignert, A.; Riget, F. Temporal Trends. In *AMAP Assessment 2002: Heavy Metals in the Arctic*, Chapter 5; Symon, C., Wilson, S. , Eds.; Arctic Monitoring and Assessment Programme: Oslo, Norway, 2005, pp 84−106.

(19) Fitzgerald, W. F.; Engstrom, D. R.; Lamborg, C. H.; Tseng, C.-M.; Balcom, P. H.; Hammerschmidt, C. R. Modern and historic atmospheric mercury fluxes in northern Alaska: Global sources and Arctic depletion. *Environ. Sci. Technol.* **2005**, *39*, 557–568.

(20) Outridge, P. M.; Sanei, H.; Stern, G. A.; Hamilton, P. B.; Goodarzi, F. Evidence for control of mercury accumulation rates in canadian high arctic lake sediments by variations of aquatic primary productivity. *Environ. Sci. Technol.* **2007**, *41*, 5259–5265.

(21) Outridge, P. M.; Stern, G. A.; Hamilton, P. B.; Percival, J. B.; McNeely, R.; Lockhart, W. L. Trace metal profiles in the varved sediment of an Arctic lake. *Geochim. Cosmochim. Acta* **2005**, *69*, 4881–4894.

(22) Oldfield, F.; Appleby, P. G. Empirical testing of 210Pb dating models for lake sediments. In *Lake Sediments and Environmental History*; Haworth, E. Y.; Lund, J. W. G. , Eds.; University of Minnesota Press: Minneapolis, MN, 1984; pp 93−124.

(23) Dastoor, A. P.; Davignon, D.; Theys, N.; Van Roozendael, M.; Steffen, A.; Ariya, P. A. Modeling dynamic exchange of gaseous elemental mercury at polar sunrise. *Environ. Sci. Technol.* **2008**, *42*, 5183–5188.

(24) Gubala, C. P.; Engstrom, D. R.; White, J. R. Effects of iron cycling on 210 Pb dating of sediments in an Adirondack lake, U.S.A. *Can. J. Fish. Aquat. Sci.* **1990**, *47*, 1821–1829.

(25) Gallon, C.; Tessier, A.; Gobeil, C. Alfaro-De La Torre M. C., Modeling diagenesis of lead in sediments of a Canadian Shield lake. *Geochim. Cosmochim. Acta* **2004**, *68*, 3531–3545.

(26) Lindeberg, C.; Bindler, R.; Renberg, I.; Emteryd, O.; Karlsson, E.; Anderson, N. J. Natural fluctuations of mercury and lead in Greenland lake sediments. *Environ. Sci. Technol.* **2006**, *40*, 90–95.

(27) Lockhart, W. L.; Wilkinson, P.; Billeck, B. N.; Danell, R. A.; Hunt, R. V.; Brunskill, G. J.; Delaronde, J.; St Louis, V. Fluxes of mercury to lake sediments in central and northern Canada inferred from dated sediment cores. *Biogeochem.* **1998**, *40*, 163–173.

(28) Michelutti, N.; Douglas, M. S. V.; Smol, J. P. Diatom response to recent climatic change in a high arctic lake (Char Lake, Cornwallis Island, Nunavut). *Global Planet. Change* **2003**, *38*, 257–271.

(29) Smol, J. P.; Douglas, M. S. V. Crossing the final ecological threshold in high Arctic ponds. *Proc. Nat. Acad. Sci. U. S. A.* **2007**, *104*, 12395–12397.

(30) Bindler, R.; Renberg, I.; Appleby, P. G.; Anderson, N. J.; Rose, N. L. Mercury accumulation rates and spatial patterns in lake sediments from West Greenland: A coast to ice margin transect. *Environ. Sci. Technol.* **2001**, *35*, 1736–1741.

(31) Gälman, V.; Rydberg, J.; De-Luna, S. S.; Bindler, R.; Renberg, I. Carbon and nitrogen loss rates during aging of lake sediment: Changes over 27 years studied in varved lake sediment. *Limnol. Oceanogr.* **2008**, *53*, 1076–1082.

(32) Lorey, P. M.; Driscoll, C. T. Historical trends of mercury deposition in Adirondack lakes. *Environ. Sci. Technol.* **1999**, *33*, 718–722.

(33) Lucotte, M.; Mucci, A.; Hillaire-Marcel, C.; Pichet, P.; Grondin, A. Anthropogenic mercury enrichment in remote lakes of Northern Québec (Canada). *Water Air Soil Pollut.* **1995**, *80*, 467–476.

(34) Engstrom, D. R.; Swain, E. B.; Henning, T. A.; Brigham, M. E.; Brezonik, P. L. In *Environmental Chemistry of Lakes and Reservoirs*; Baker, L. A. , Eds.; American Chemical Society: Washington, DC, 1994; pp 33−66.

(35) Grigal, D. F. Inputs and outputs of mercury from terrestrial watersheds: A review. *Environ. Rev.* **2002**, *10*, 1–39.

(36) Lindeberg, C.; Bindler, R.; Renberg, I.; Emteryd, O.; Karlsson, E.; Anderson, N. J. Natural fluctuations of mercury and lead in Greenland lake sediments. *Environ. Sci. Technol.* **2006**, *40*, 90–95.

(37) Pacyna, E.; Pacyna, J.; Steenhuisen, F.; Wilson, S. Global anthropogenic mercury emission inventory for 2000. *Atmos. Environ.* **2006**, *40*, 4048–4063.

(38) Engstrom, D. R.; Swain, E. B. Recent declines in atmospheric mercury deposition in the upper Midwest. *Environ. Sci. Technol.* **1997**, *31*, 960–967.

(39) Brooks, S.; Lindberg, S.; Gordeev, V.; Christensen, J.; Gusev, A.; Macdonald, R.; Marcy, S.; Puckett, K.; Travnikov, O.; Wilson, S. Transport pathways and processes leading to environmental exposure. In *AMAP Assessment 2002 Heavy Metals in the Arctic*, Chapter 3; Symon, C., Wilson, S. J., Eds.; Arctic Monitoring and Assessment Programme (AMAP): Oslo, Norway, 2005, pp 11−41.
(40) Shotyk, W.; Zheng, J.; Krachler, M.; Zdanowicz, C.; Koerner, R.; Fisher, D. Predominance of industrial Pb in recent snow (1994−2004) and ice (1842−1996) from Devon Island, Arctic Canada. *Geophys. Res. Let.* **2005**, *32*, 1–4.
(41) Temme, C.; Blanchard, P.; Steffen, A.; Banic, C.; Beauchamp, S.; Poissant, L.; Tordon, R.; Wiens, B. Trend, seasonal and multivariate analysis study of total gaseous mercury data from the Canadian atmospheric mercury measurement network (CAMNet). *Atmos. Environ.* **2007**, *41*, 5423–5441.
(42) Boutron, C. F.; Vandal, G. M.; Fitzgerald, W. F.; Ferrari, C. P. A forty year record of mercury in central Greenland snow. *Geophys. Res. Let.* **1998**, *25*, 3315–3318.
(43) Brooks, S.; Saiz-Lopez, A.; Skov, H.; Lindberg, S.; Plane, J.; Goodsite, M. The mass balance of mercury in the springtime arctic environment. *Geophys. Res. Let.* **2006**, *33*, L13812.
(44) U.S. EPA. Mercury Study Report to Congress; EPA-452-97-003-010. Volume III: Fate and Transport of Mercury in the Environment; United States Environmental Protection Agency, Office of Air and Radiation: Washington, DC, 1997.
(45) Gbor, P. K.; Wen, D.; Meng, F.; Yang, F.; Sloan, J. J. Modeling of mercury emission, transport and deposition in North America. *Atmos. Environ.* **2007**, *41*, 1135–1149.
(46) St Louis, V. L.; Sharp, M. J.; Steffen, A.; May, A.; Barker, J.; Kirk, J. L.; Kelly, D. J. A.; Arnott, S. E.; Keatley, B.; Smol, J. P. Some sources and sinks of monomethyl and inorganic mercury on Ellesmere island in the Canadian high arctic. *Environ. Sci. Technol.* **2005**, *39*, 2686–2701.
(47) Garbarino, J. R.; Snyder-Conn, E.; Leiker, T. J.; Hoffman, G. L. Contaminants in arctic snow collected over northwest Alaskan sea ice. *Water Air Soil Pollut.* **2002**, *139*, 183–214.
(48) Constant, P.; Poissant, L.; Villemur, R.; Yumvihoze, E.; Lean, D. Fate of inorganic mercury and methyl mercury within the snow cover in the low arctic tundra on the shore of Hudson Bay (Québec, Canada). *J. Geophys. Res., [Atmos.]* **2007**, 112.

ES8035412

Supporting information

Spatial Trends and Historical Deposition of Mercury and Lead in Eastern and Northern Canada Inferred from Lake Sediment Cores

D.C.G. Muir [1]*, X. Wang[1], F. Yang[1], N. Nguyen[1], T.A. Jackson[1], M.S. Evans[2], M. Douglas[3], G. Köck[4], S. Lamoureux[5], R. Pienitz[6], J.P. Smol[7], W.F. Vincent[6] and A. Dastoor[8]

[1]Environment Canada, Aquatic Ecosystem Protection Research Division, Burlington ON L7R 4A6
[2]Environment Canada, Aquatic Ecosystem Protection Research Division, Saskatoon, SK S7N 3H5
[3] Canadian Circumpolar Institute, University of Alberta, Edmonton, AB T6G 2R3
[4] Austrian Academy of Sciences, Dr. Ignaz Seipel-Platz 2, A-1010 Vienna, Austria
[5] Dept. of Geography, Queen's University, Kingston ON K7L 3N6
[6] Centre d'Etudes Nordiques, Université Laval, Québec Qc G1V 0A6
[7] Dept. of Biology, Queen's University, Kingston ON K7L 3N6
[8] Environment Canada, Air Quality Research Division, Dorval, QC H9P 1J3

Table of Contents **pg**

lake from the nearest ocean waters.

References **25**

1. **Additional sample collection and analysis information**

Objective: Sediment cores were obtained during the period 1998-2005. The objective was a north-south transect from northeastern USA to Ellesmere Island and a west-east transect from southwestern Northwest Territories (NWT) to Labrador. Logistical constraints (e.g. the need to access all Arctic and subarctic lakes by air) limited systematic geographical coverage.

Lake characteristics: Of the 50 lakes, 42 had completely uninhabited catchments, 5 had some habitation (generally cottages) and 3 had small municipalities (Nipigon, Big Trout, Superior). Some large subarctic lakes e.g. Big Trout, Fisherman, Shipiskan have important First Nations subsistence fisheries and therefore some light boat traffic. Two mid-latitude lakes, Nipigon and Superior have municipal waste treatment sources, but are thought to receive most inputs of pollutants from the atmosphere [1]. Most small mid-latitude lakes were undisturbed and located in Parks (Connery, Opeongo), next to Research facilities (Plastic, Cromwell, Croche, Batchewana), or undisturbed private land (Bates, Dufferin, St. George, Philips).

Sample collection: Cores were obtained with KB (Kajak-Brinkhurst type corer [2, 3], Glew [4] or Uwitec (Uwitec, Mondsee, Austria) corers using 6-10 cm diameter acrylic plastic tubes. All cores, except Lakes A, Cli, Croche, Cromwell, Connelly, Hazen, North and West were obtained in July-September from a small boat or a float-equipped aircraft**.** The latter 6 were obtained through holes drilled through the ice. Multiple cores were obtained at each site. The deepest point in each lake were selected by sonar, or using bathymetric maps, avoiding steep sloped areas that might be subject to slumping. Cores were extruded and sliced into 0.5 or 1 cm sections (SI Table S1) Sediments were stored in WhirlPak^{R} polyethylene bags or in wide-mouth polypropylene jars. Sediments were kept in cool dark storage during the field work and then shipped by air freight to the laboratory where they were stored in the dark at 4°C.

Core Dating: Sediment cores were dated using the ^{210}Pb and/or ^{137}Cs methods, and sedimentation rates and dates were estimated using the Constant Rate of Supply (CRS) model [5]. Freeze-dried subsamples of each section were treated using a variation on the Eakins and Morrison [6] polonium distillation procedure. Single cores from each lake were dated except for Lakes Siskiwit, Shipiskan, Char, Cli, and Amituk, where 2 cores taken the same year or within 4 years, were dated. Only cores with interpretable ^{210}Pb or ^{137}Cs stratigraphy were selected for analysis; they typically yielded 10-20 post-1800 core sections or horizons, per core. One core (Lake A in northern Ellesmere Island) was dated by counting annual laminations (varves) in another core taken at the same location, due to low ^{210}Pb and ^{137}Cs values. A sedimentation rate was not estimated for Lake A.

Excess ^{210}Pb activity was low in high latitude cores. ^{210}Pb deposition declines exponentially with latitude and, in North America (See Figure S2), is about 5-fold lower at 60^{o}N than at 30^{o}N because of lower precipitation at higher latitudes [7, 8]. In the High Arctic permafrost may reduce radon gas (the parent of ^{210}Pb) emissions from soil and extended periods of ice cover may prevent atmospheric ^{210}Pb from reaching lake sediments [8, 9].

Sediment particle focussing factors (FF) were estimated for all cores dated by dividing the observed ^{210}Pb flux (Bq m^{-2}y^{-1}) by the predicted ^{210}Pb flux for the same latitude based on soil ^{210}Pb measurements from 41.5 to 81.5 degrees latitude. This method was previously used in a study of latitudinal gradients of PCBs [10] and is discussed in detail in an unpublished study [11]. The regression of soil ^{210}Pb fluxes vs latitude shown in Figure S1 is derived from that study.

Mercury and multi-element analysis: In all, 50 dated cores were available for detailed analysis. Freeze dried subsamples were placed in Teflon® vessels acid-digested with a mixture of nitric and hydrochloric acids and hydrogen peroxide (ratio 9:2:1) in a high pressure microwave oven. Total Hg was determined by cold vapour atomic absorption spectrometry. A subset of cores were analysed by direct combustion using a DMA-80 (Milestone Instruments, Shelton, CT). Total Pb, manganese (Mn) and iron (Fe) were determined in 48 of 50 cores. Pb was determined by inductively coupled plasma-mass spectrometry (ICP-MS) (PQ-2, VG Elemental) and Mn and Fe using ICP-atomic emission spectrometry (AES). A subset of the cores (15) were analysed for "reactive" Fe and Mn by extraction with 1 M HCl [12]), and the extracts were analysed by ICP-AES. Multielement analysis for between 10 and 30 additional trace elements was conducted by ICP-MS on 38 of 50 cores. Organic carbon was determined by CHN analyser in subsamples from 47 of 50 cores. Certified sediment reference materials (NRC MESS-3 and NIST RM 8704) were used to ensure accuracy. Results for Hg were consistently within ±7% of certified values by cold vapour atomic absorption spectrometry and within ±5% for DMA analysis. All the ICP-MS and CHN analyses were performed at the National Laboratory for Environmental Testing (NLET, Burlington ON).

Hg concentrations have been previously reported for the same cores from three of the study lakes. He et al. [13] reported results for Hg and methyl Hg in lakes St. George and Philips. Jackson et al. [14] reported Hg concentrations in a core from Romulus Lake and Jackson et al. [15] reported concentrations of Hg in the surface sections of cores from Lakes Cli and Shipiskan.

For several lakes e.g. Amituk, Char, Hazen, Plastic, Siskiwit here have been multiple cores dated either by our lab or in other studies. For example Lockhart et al [16] reported sedimentation rates for lakes Amituk and Hazen which are in good agreement with this study after focus correction. Our own multiple cores from Char and Siskiwit Lake show agreement in CRS model sedimentation rates within 10% (data not shown). Mills et al [17] reported a sedimentation rate for Plastic Lake (97 g m^{-2} yr^{-1}) which is in good agreement with ours (120 g m^{-2} yr^{-1}) after correction for focussing.

2. Profiles of other elements:

The concentration profiles of total Fe and Mn also showed a tendency to increase towards the surface i.e. significant positive (+) and negative (-) correlations with year of deposition (SI Figure S3), although, generally not in parallel with Hg concentrations which frequently peaked in sub-surface horizons. "Reactive" Fe and Mn profiles were examined in 15 of the lakes. Both were strongly correlated with total Fe and Mn and therefore only the latter measurements were done on the 34 other cores (data not shown). The lack of a consistent trend of Fe and Mn with Hg confirms previous conclusions suggesting a lack of any major effects of diagenetic processes on Hg vertical movement in sediments [18] .

Results for Al were available for 33 cores and showed much less variation with deposition year than Hg concentrations (SI Table S3). Al concentrations had significant + and - correlations with sedimentation rate in a relatively small number of lakes (4 of 20 Arctic and subarctic) compared with Hg. Al was + correlated with Hg in only 4 lakes and negatively correlated in 14 of 33. Al and Zn were + correlated in 12 of 14 Arctic lakes but only in 1 of 14 mid-latitude lakes. Outridge et al [19] also found significant correlations between Al and Zn, as well as between Al and Hg, in a core from a small lake on Devon Island (DV-09) post -1854 stratigraphy and attributed a significant fraction of Hg input to local geological sources via weathering and runoff from melting snow.

3. Comparison with model predictions

The Danish Eulerian Hemispheric model (DEHM) predicts annual Hg deposition with Hg depletion events ranging from >18 μg m^{-2} y^{-1} in eastern North America to 6-12 μg m^{-2} y^{-1} in the Canadian Arctic archipelago [20]. With MDE omitted the estimated Hg deposition was predicted to decline more sharply from >18 μg m^{-2} y^{-1} in southern Ontario and Québec to <3-6 μg m^{-2} y^{-1} in the archipelago. Modelling of total wet + dry deposition estimated for the northeastern US and adjacent areas of southern Canada showed a latitudinal decline from 10-30 ug/m^2 in upper New York State, Vermont and southern Ontario (43-45 ^{o}N) to 3-10 ug/m^2 at 46-48 ^{o}N range and 0.3-1 μg /m^2 at 51-53 ^{o}N [21]. Gbor et al [22] using the EPA SMOKE/CMAQ modeling system predicted higher deposition ranging from 30-40 ug/m^2 in upper New York State to 10-20 ug/m^2 at 51-53 ^{o}N. Using the Environment Canada Global/regional atmospheric heavy metals (GRAHM) model, Dastoor and Larocque [23] showed dry deposition over this same region declining from about 10-20 ug/m^2 to 0.5-1 μg /m^2 while summertime wet deposition was estimated to be more variable latitudinally in Eastern North America ranging from 2-20 μg /m^2.

Dastoor et al. [24] have modeled the deposition of Hg to the Arctic Ocean including MDEs and associated atmospheric chemistry pathways. They estimated Hg deposition in the western Canadian Arctic archipelago of 20-35 μg m^{-2} y^{-1} with maximum deposition occurring in March – May as a result of MDEs. About 40% was estimated to be re-emitted. The current version of GRAHM used for this study takes revolatilization into account and predicted Hg fluxes of 4, 11 and 22 μg m^{-2} y^{-1} for the Arctic, Subarctic and mid-latitude lake locations, which is in very good agreement with the general trend seen for $\Delta F_{adj,F}$ and the average fluxes for each region. This agreement of modeled and measured deposition lends additional support to the hypothesis that most Hg deposited from MDEs would be revolatilized. Nevertheless the proximity of many of the lakes in the Arctic islands to the ocean might result in greater deposition over time. Constant et al. [25] observed an exponential decline of gaseous elemental Hg with distance (0.9 to 2.9 km) from Hudson Bay and Garbarino et al. [26] found higher concentrations of Hg in snow near marine areas of coastal Alaska than at inland sites. Berg et al. [27] reported higher concentrations of Hg in moss collected in the northern coast of Norway than inland, and presented evidence that this could be could partly be due to MDEs. We examined this question for the 18 Arctic and 2 subarctic lakes in this study that were within 80 km of the ocean (see Table S1 for distances). No significant trend was found between Hg FR or with $\Delta F_{adj,F}$ and log distances or square root of the distance, even after omitting the most distant lake (Figure S7).

Miller et al. [28] estimated (dry+wet) Hg deposition for rural areas of the Northeastern US and adjacent Canadian provinces ranging from about 4 to 30 μg m^{-2} y^{-1}. Deposition was predicted to be higher (25-32 μg m^{-2} y^{-1}) in the west and southwest parts of this region (north of Lake Ontario and in the Catskill Mountains north of New York) and lower (5-15 μg m^{-2} y^{-1}) in Québec north of 50^{o}N. These values are in good agreement with Hg $\Delta F_{adj,F}$'s calculated from sediment deposition.

The agreement between modeled Hg deposition and our empirical estimates is very good over the latitudinal gradient which suggests that this approach, first applied by Perry et al. [29] can be broadly utilized. However, there are uncertainties in calculation $\Delta F_{adj,F}$ which need to be recognized. The values for FF have considerable uncertainty due to the limited number of independent measurements of ^{210} Pb fluxes to soil along a north-south transect in North America (see SI Figure S2 and related equation). Uncertainties (% standard error) in estimation of the FF are about ±30%. Average sedimentation rates calculated with the CRS model have uncertainties of 20-40% based on the fit of the unsupported ^{210}Pb activity against cumulative dry weight. The analysis of multiple cores from each lake would, of course, improve the estimate of the true sedimentation rate and the FF but, except for the 4 lakes that were cored twice, this was not feasible in the present study. To reduce lake to lake variation future studies along this north south

gradient ideally should focus on a more consistent set of lakes e.g. lakes with similar areas and catchments, as well as multiple cores from each lake.

4. **Additional acknowledgements:**
We thank the following personnel at Environment Canada (Burlington ON): Camilla Teixeira, for core collection, Gina Sardella, Bert Francoeur and Jacques Carrier for metals analysis; Jessica Epp for Hg analyses by DMA, Heather Engbers for graphing of ^{210}Pb data, Charlie Talbot, Mike Mawhinney, Ross Neureuther, Dan Walsh, and Bruce Grey of Research Support Services (Burlington ON) for field support and core collection. We are grateful to the following individuals and organizations for permission to collect cores: R. Carignan, Université de Montréal, Station Biologique, New York State Dept of Environmental Conservation (for Adirondack Park), Ontario Ministry of Natural Resources for Lake Opeongo and Plastic Lake, US National Parks Service for Siskiwit Lake (Isle Royale), Parks Canada for cores in Nahanni, Quttinirpaaq, Sirmilik and Tuktut Nogait National Parks, the Acho Dene Koe First Nations (Fort Liard NWT) for a core from Fisherman Lake, and the Innu Nation (Goose Bay NF) for collection at Shipiskan Lake. We thank Alex Wolfe (University of Alberta) for providing a core (CF-11) from Clyde River NU, Julia Lu, Ryerson University, for Hg data for cores from Lakes Phillips and St George. We thank Jessica Tomkins (Queen's University) for providing the varve chronology for the Lake A core.

Table S1. Information on the 50 Arctic, subarctic and mid-latitude lakes and sediment characteristics

Region	Lake/core	Loca-tion	Lat °N	Long °W	Precip [1] (mm)	Collection group[2]	Slice thick-ness (cm)	Yr collected	Distance from ocean (km)	A_L[3] km^2	A_C/A_L	FF[4]	Sed rate[5] g $m^{-2}y^{-1}$	change in sed rate %[6]	Al ratio[7]	Zn ratio[8]	% Org carbon[9]	OC ratio[10]
Arctic	A (Ellesmere)	NU	83.0	70.5	154	Vincent	1.0	2001	12	4.9	7.4		[6]					
Arctic	Amituk	NU	75.0	93.8	150	Kock	0.5	2002	5.3	0.38	69.1	3.67	260	28	1.32	1.45	5.4	1.362
Arctic	AXAJ	NU	80.0	87.0	76	Douglas/Smol	0.5	1998	5.7	0.1	21.1	0.55	110	110				
Arctic	BI-02	NU	73.0	80.0	191	Pienitz	0.5	2005	0.35	0.033	9.2	0.87	200	-10	0.92	0.95	9.6	1.025
Arctic	BK-AH	NU	73.4	119.4	149	Douglas/Smol	0.5	2000	46	0.01	1.4	1.29	20	-71	0.18	0.23	12.7	1.168
Arctic	CF11-G1	NU	70.3	68.4	233	Wolfe	0.5	2002	2.6	0.094	5	1.54	100	100	1.92	1.92	2.8	1.114
Arctic	Char	NU	74.6	94.8	150	NWRI	0.5	2003	1.6	0.53	8.2	3.11	240	192	2.59	2.83	2.2	1.225
Arctic	DVE	NU	75.3	89.5	150	Douglas/Lim	0.5	2001	5.3	0.01	24	0.47	130	-8	0.94	0.93	8.7	0.905
Arctic	Hazen	NU	82.0	70.0	154	NWRI	0.5	2005	80	538	9.1	1.20	498	0	1.24	0.97	1.8	0.971
Arctic	MB-AC	NU	76.2	119.2	111	Douglas/Smol	0.5	1999	1.5	0.001	14.3	0.71	330	-41	0.52	0.51	2.5	1.468
Arctic	MBS	NU	76.1	119.2	111	Douglas/Smol	0.5	1999	0.75	0.001	8	0.60	220	-2	0.60	0.87	5.0	1.045
Arctic	North	NU	74.8	90.1	150	Lamoureux	0.5	2005	1.8	0.59	165	6.32	1000	32	1.81	1.93	3.6	1.692
Arctic	Rocky Basin	NU	78.4	77.5	76	Douglas/Smol	0.5	1998	3	0.038	23.8	0.73	10	0			6.8	1.937
Arctic	Romulus	NU	79.5	85.1	76	Vincent	1.0	2000	6.6	4.4	4.6	5.05	820	10		1.07	8.0	1.409
Arctic	Rummy	NWT	69.0	122.3	157	EC/Halliwell	1.0	1999	28	1.91	45.1	1.94	79	1			2.2	2.152
Arctic	SHI-L4	NU	65.0	83.8	286	NWRI	0.5	2001	6	0.085	189	1.76	300	48	1.28	1.21	5.2	1.874
Arctic	SHI-L7	NU	65.2	84.2	286	Pienitz	0.5	2004	3.6	0.041	70.7	0.36	60	10	1.01	1.09	1.8	0.959
Arctic	West	NU	74.9	109.7	111	Lamoureux	0.5	2003	3.6	1.12	12.9	1.69	430	128	2.20	2.19	1.5	1.101
Subarctic	B2-1	QC	57.5	76.1	460	Pienitz	0.5	2000	40	0.033	2	1.20	160	23		0.99	10.1	
Subarctic	Big Trout	ON	53.5	89.5	609	NWRI	1.0	2001	>80	675	5.6	0.57	130	0	1.34	1.40	9.3	1.057
Subarctic	Cli	NWT	62.0	122.0	290	Evans	1.0	2001	>80	3	1.8	2.17	212	-16	0..98	0.97	3.0	0.936
Subarctic	Fisherman	NWT	60.2	123.6	369	EC/Halliwell	0.5	2001	>80	11	30.3	0.17	310	14	0.91	0.89	2.8	1.098
Subarctic	Kachishayoot	QC	55.2	77.4	649	Vincent	1.0	1999	4	0.3	6	1.03	60	-25			16.7	1.283
Subarctic	Merrick	MB	55.3	93.0	499	NWRI	1.0	2001	>80	6.9	4.8	0.33	110	150	2.43	3.39	39.9	1.276
Subarctic	Minipi	NFLB	52.2	60.4	949	NWRI	1.0	2001	>80	97	29.6	0.11	30	50	1.45	1.24	5.6	0.998
Subarctic	Mista	MB	55.5	93.0	499	NWRI	1.0	2001	>80	10	3.8	0.19	40	-43	0.42	0.44	37.5	1.732
Subarctic	Oksana	QC	54.5	66.5	823	Pienitz	1.0	1999	>80	2	2.2	0.66	50	14			28.5	1.024
Subarctic	Q27	QC	53.2	77.3	684	Pienitz	1.0	2001	>80	0.61	5.6	0.81	90	125	1.40	3.36	15.0	1.288
Subarctic	Q6	QC	51.1	77.3	906	Pienitz	1.0	2001	>80	0.057	4.8	0.76	60	30	1.53	3.47	13.2	1.143
Subarctic	Rabbitkettle	NWT	61.3	126.0	369	EC/Halliwell	0.5	2000	>80	0.63	4.9	0.57	250	49		1.17	7.3	1.425
Subarctic	Shipiskan	NFLB	54.5	62.2	823	NWRI	1.0	2004	>80	50	138	3.11	190	6	0.94	1.08	6.3	2.543
Subarctic	TK-54	NWT	64.3	112.4	303	Douglas/Smol	1.0	1998	>80	0.099	4.2	2.16	97	223				0.549
Mid-lat	Batchawana	ON	45.8	82.6	1215	NWRI	1.0	2000	>80	0.058	13.7	0.60	60	-33	0.57	1.93	19.1	0.941
Mid-lat	Bates	CT	41.6	72.0	1302	Pienitz	1.0	2001	>80	0.027	22.2	0.29	170	200	2.85	1.72	12.1	1.153
Mid-lat	Britt Brook	NB	47.0	66.8	1134	NWRI	1.0	1999	>80	1.07	16.5	0.32	80	100			16.2	1.000
Mid-lat	Connery	NY	44.3	73.8	1012	NWRI	1.0	2001	>80	0.33	6.1	0.44	140	40	1.29	2.22	11.9	1.126

Mid-lat	Croche	QC	46.0	74.0	1164	NWRI	1.0	2001	>80	0.17	4.9	0.59	140	40	1.20	2.09	22.7	1.155
Mid-lat	Cromwell	QC	46.0	74.0	1164	NWRI	1.0	2001	>80	0.14	98.2	0.10	40	33	1.28	1.47	22.8	1.361
Mid-lat	Dasserat	QC	48.3	79.5	884	NWRI	1.0	2000	>80	26.7	23.3	0.90	470	292		5.24	3.2	1.075
Mid-lat	Dufferin	ON	43.8	80.0	892	NWRI	0.5	2004	>80	0.05	12.6	0.51	170	148	3.07	2.02	12.1	0.981
Mid-lat	Eva	ON	49.8	92.7	740	NWRI	1.0	2000	>80	1708	4.3	0.37	270	29	1.29	2.00	7.2	1.129
Mid-lat	Levi	VT	44.2	72.2	979	Pienitz	1.0	1998	>80	0.09	4.9	0.26	90	125	2.36	3.06	20.4	0.974
Mid-lat	Nipigon	ON	49.6	88.3	760	NWRI	0.5	1998	>80	4848	4.5	0.44	200	0			2.1	1.179
Mid-lat	Opeongo	ON	45.3	78.3	1032	NWRI	0.5	1998	>80	58.6	5.2	1.16	120	-70	0.88	2.01	8.3	1.072
Mid-lat	Philips	ON	43.9	79.5	892	NWRI	1.0	2005	>80	0.094	5.9	0.48	150	3			15.0	1.053
Mid-lat	Plastic	ON	45.2	78.8	1032	NWRI	1.0	2004	>80	0.32	2.5	0.41	50	-36	0.50	1.37	20.0	1.054
Mid-lat	Siskiwit	MI	48.0	88.7	789	NWRI	0.5	2005	>80	16.8	3.1	0.95	150	107	1.56	2.64	7.1	1.680
Mid-lat	StGeorge	ON	44.0	79.4	892	NWRI	1.0	2005	>80	0.11	14.5	0.38	240	14			15.0	1.253
Mid-lat	Superior	ON	46.9	86.5	789	NWRI	0.5	2001	>80	82170	0.6	2.53	140	0	0.85	1.48	2.5	0.598
Mid-lat	Thunder	ON	49.7	91.1	740	NWRI	1.0	2000	>80	1123	10.9	0.48	220	-5	0.88	1.02	3.6	0.680

[1] Average annual precipitation for each location based on the nearest Environment Canada or NOAA weather station

[2]Collection group that conducted the field work. W. Vincent (Univ. Laval); R. Pienitz (Univ. Laval), M. Douglas/D. Lim (U of Toronto), J. Smol (Queen's Univ.), EC/Halliwell = D. Halliwell (EC Prairie and Northern Region); NWRI = EC Research Support Division; Wolfe = A. Wolfe (Univ of Alberta).

[3]LA = lake area (km^2)

[4]FF=focusing factor.

[5] Sedimentation rate estimated using the CRS model based on excess ^{210}Pb except for Lakes A and Hazen. For Lake Hazen the sedimentation rate reported by Muir et al [10] was used. No sedimentation rate could be estimated for Lake A.

[6] % change in recent sedimentation rate (post-1990) compared to pre-1850 rate

[7]Al ratio = Al concentration in recent horizons (post-1990) divided by pre-1850 concentration

[8]Zn ratio = Zn concentration in recent horizons (post-1990) divided by pre-1850 concentration

[9]% Org carbon (OC) = % organic carbon of recent horizons

[10]OC ratio = % OC in recent horizons (post-1990) divided by % OC of pre-1900 horizons

Table S2. Soil measurements of ^{210}Pb fluxes used for developing a relationship between ^{210}Pb deposition and latitude[1]. Results are from Omelchenko et al [11] except for reference [30].

Location	Latitude	Longitude	Bq m^{-2} y^{-1}	Reference	
Steam Mill, PA	41.5	78	150	Nozaki et al 1978	[31]
Branch Pond VT	44	73	283	Davis et al 1984	[32]
Lake Ontario	43.5	77	250	Eisenreich et al. 1989	[33]
Crystal Lake, WI	46	89.6	259	Talbot and Andren 1983	[34]
ELA, ON	49.5	93.5	175	Lockhart et al 1998	[16]
Trout Lake, ON	51.2	93	160	Lockhart et al 1998	[16]
Lake Laberge, YK	61.2	135	80	Lockhart et al 1998	[16]
Saqvaqjuac, NU	63.6	90.6	60	Lockhart et al 1998	[16]
Lac Belot, NWT	66.5	126	50	Lockhart et al 1998	[16]
Devon Is., NU	75	89	27	Lockhart et al 2000	[16]
Camp century Greenland	77	61	15	Turekian et al. 1977	[35]
Site 2, Greenland glacier	77	56	18	Turekian et al. 1977	[35]
Lake Hazen, NU	81.5	71.3	7	Lockhart et al 1998	[16]
Toolik lakes, AK	68.8	150	30.4	Fitzgerald et al. 2005	[30]

[1]Regression of log ^{210}Pb flux vs latitude yields:
Log ^{210}Pb = 3.95±0.16 – 0.0352±0.0026*latitude, R^2=0.939

Table S3. Numbers and percent of lakes with significant relationships of Hg, Fe, Mn, Al, organic carbon and sedimentation rate with deposition year and with each other[1].

		+ or – relationship	Number with significant r values			% with significant correlations		
Parameter			Arctic	Subarctic	mid-latitude	Arctic	subarctic	mid-latitude
	N >>>		17	14	18	%	%	%
Hg	Year[2]	+	13	12	18	76	86	100
		-	0	1	0			
Fe	year	+	2	5	10	12	36	56
		-	3	0	3			
Mn	year	+	6	10	7	35	71	39
		-	3	0	4			
Sedrate	year	+	8	7	12	47	50	67
		-	2	2	4			
Hg	Fe	+	3	6	12	18	43	67
		-	1	0	0			
Hg	Mn	+	6	6	8	35	43	44
		-	3	2	5			
Mn	Fe	+	8	7	9	47	50	50
		-	0	0	3			
Sed rate	Hg	+	5	5	9	29	36	50
		-	2	1	1			
Sed rate	Fe	+	1	3	8	6	21	44
		-	3	0	2			
Sed rate	Mn	+	7	6	10	41	43	56
		-	2	1	0			
	N >>>		11	9	13	%	%	%
Al	year	+	2	2	8	12	14	44
		-	2	2	0			
Hg	Al	+	2	0	2	12	0	11
		-	2	3	9			
Sed rate	Al	+	0	2	4	0	14	22
		-	1	2	1			
	N >>>		14	9	14			
Zn	Year	+	4	2	8	29	22	57
		-	2	2	1			
Zn	Al	+	12	2	1	86	22	7
		-	0	1	4			
Sed rate	Zn	+	2	2	5	14	22	36
		-	2	2	1			
	N >>>		15	14	17	%	%	%
OC	year	+	6	3	6	35	21	33
		-	0	2	3			
Hg	OC	+	4	3	8	24	21	44
		-	1	0	1			
Sed rate	OC	+	4	5	6	24	36	33
		-	0	0	0			

[1]Pearson correlation coefficients by lake significant at $P<0.05$ (uncorrected probabilities)
[2]Year = median date for each sediment core section assigned by the CRS model

Table S4. Sediment cores from 50 Arctic, subarctic and mid-latitude lakes collected 1998-2005, including surface mercury concentrations (μg/g dry wt), fluxes (μg m^{-2} y^{-1}) and flux ratios and predicted fluxes for mercury using GRAHM

Region	Lake/core	Location	Lat °N	Long °W	Mercury[1]				Mercury			GRAHM
					Conc'n	Max[2]	Max[2]	FR[3]	--------- Adjusted ----------			Model
					μg/g surface	Sub-surface flux	Sub-surface conc'n		Recent Flux[4]	Pre-ind flux[4]	$\Delta F_{adj,F}$[5]	Predicted flux
Arctic	A (Ellesmere)	NU	83.0	70.5	0.10	-	N	1.92	[7]			4.3
Arctic	Amituk	NU	75.0	93.8	0.05	N	Y	2.42	3.3	1.3	1.54	3.6
Arctic	AXAJ	NU	80.0	87.0	0.28	N	N	3.00	53.6	17.9	16.1	2.2
Arctic	BI-02	NU	73.0	80.0	0.05	N	N	1.68	9.6	5.7	3.88	3.6
Arctic	BK-AH	NU	73.4	119.4	0.10	Y	N	0.50	1.5	3.0	-1.53	3.6
Arctic	CF11-G1	NU	70.3	68.4	0.03	N	N	4.14	1.9	0.45	0.97	4.9
Arctic	Char	NU	74.6	94.8	0.03	N	Y	4.55	2.0	0.43	0.70	4.0
Arctic	DVE	NU	75.3	89.5	0.02	N	N	1.05	4.4	4.2	0.21	4.0
Arctic	Hazen	NU	82.0	70.0	0.07	N	N	1.13	27.6	24.5	3.11	3.1
Arctic	MB-AC	NU	76.2	119.2	0.03	Y	N	0.79	9.7	12.3	-2.61	3.7
Arctic	MBS	NU	76.1	119.2	0.02	N	N	1.20	6.6	5.5	1.11	3.7
Arctic	North	NU	74.8	90.1	0.02	N	N	3.09	2.3	0.75	1.33	4.3
Arctic	Rocky Basin	NU	78.4	77.5	0.25	N	N	2.76	3.4	1.2	2.18	5.2
Arctic	Romulus	NU	79.5	85.1	0.05	Y	Y	1.67	11.1	6.6	3.80	2.3
Arctic	Rummy	NWT	69.0	122.3	0.10	N	N	1.58	3.9	2.5	1.40	5.6
Arctic	SHI-L4	NU	65.0	83.8	0.07	N	N	2.89	11.8	4.1	5.79	6.0
Arctic	SHI-L7	NU	65.2	84.2	0.16	N	N	1.50	25.8	17.2	6.89	5.8
Arctic	West	NU	74.9	109.7	0.06	N	N	2.92	15.0	5.0	3.48	3.6
Subarctic	B2-1	QC	57.5	76.1	0.12	Y	Y	2.33	16.2	6.9	7.64	7.9
Subarctic	Big Trout	ON	53.5	89.5	0.11	N	N	2.65	25.0	9.4	15.6	13.6
Subarctic	Cli	NWT	62.0	122.0	0.09	N	N	1.48	9.0	6.1	2.92	7.5
Subarctic	Fisherman	NWT	60.2	123.6	0.05	N	N	1.39	86.0	61.9	15.5	9.5
Subarctic	Kachishayoot	QC	55.2	77.4	0.14	N	N	1.32	6.8	5.2	1.63	8.7
Subarctic	Merrick	MB	55.3	93.0	0.11	N	N	3.88	32.1	8.3	11.4	12.7
Subarctic	Minipi	NFLB	52.2	60.4	0.14	N	N	5.07	38.7	7.6	27.3	14.3
Subarctic	Mista	MB	55.5	93.0	0.10	N	N	1.63	21.7	13.3	8.37	12.2
Subarctic	Oksana	QC	54.5	66.5	0.21	Y	Y	1.12	14.7	13.1	-0.28	10.9
Subarctic	Q27	QC	53.2	77.3	0.15	N	N	4.71	14.9	3.2	7.76	12.4
Subarctic	Q6	QC	51.1	77.3	0.22	Y	Y	1.27	18.1	14.2	-0.38	17.2
Subarctic	Rabbitkettle	NWT	61.3	126.0	0.13	N	Y	1.07	57.5	53.9	-22.9	9.1
Subarctic	Shipiskan	NFLB	54.5	62.2	0.21	N	N	2.81	12.5	4.5	7.82	10.0
Subarctic	TK-54	NWT	64.3	112.4	0.07	Y	Y	4.22	3.6	0.85	0.85	5.2
Mid-lat	Batchawana	ON	45.8	82.6	0.46	N	N	1.04	46.3	44.4	1.84	19.6
Mid-lat	Bates	CT	41.6	72.0	0.31	N	N	4.16	148.9	35.8	41.6	20.2
Mid-lat	Britt Brook	NB	47.0	66.8	0.16	N	N	5.69	39.3	6.9	25.5	19.6
Mid-lat	Connery	NY	44.3	73.8	0.24	N	N	2.05	76.2	37.1	24.2	23.1
Mid-lat	Croche	QC	46.0	74.0	0.28	N	N	2.49	65.5	26.3	28.6	20.8
Mid-lat	Cromwell	QC	46.0	74.0	0.30	N	N	1.48	121.0	81.7	12.1	20.8
Mid-lat	Dasserat	QC	48.3	79.5	0.15	N	N	8.52	77.9	9.1	42.1	19.6
Mid-lat	Dufferin	ON	43.8	80.0	0.07	Y	N	6.05	40.1	6.6	23.7	28.1
Mid-lat	Eva	ON	49.8	92.7	0.18	N	N	3.47	47.3	13.6	29.8	18.4
Mid-lat	Levi	VT	44.2	72.2	0.23	Y	Y	4.53	80.3	17.7	40.4	22.5
Mid-lat	Nipigon	ON	49.6	88.3	0.09	Y	Y	1.95	38.5	19.8	18.7	17.5
Mid-lat	Opeongo	ON	45.3	78.3	0.82	N	N	7.68	70.4	9.2	61.2	24.6
Mid-lat	Philips	ON	43.9	79.5	0.19	N	N	2.31	60.8	26.4	33.6	28.8
Mid-lat	Plastic	ON	45.2	78.8	0.29	N	N	1.71	31.2	18.3	12.9	26.2
Mid-lat	Siskwit	MI	48.0	88.7	0.14	Y	Y	3.53	26.9	7.6	11.1	17.4
Mid-lat	StGeorge	ON	44.0	79.4	0.18	N	N	1.84	120.3	65.6	45.6	28.8
Mid-lat	Superior	ON	46.9	86.5	0.11	Y	Y	3.32	6.0	1.8	4.18	17.5

Mid-lat	Thunder	ON	49.7	91.1	0.10	N	N	2.28	45.6	20.0	25.6	20.0
Avg or GM	Arctic				0.08	18%	17%	2.17	11.4	6.6	2.8	4.1
Avg or GM	Subarctic				0.13	25%	33%	2.50	25.5	14.9	5.9	10.7
Avg or GM	Mid-latitude				0.24	28%	22%	3.56	63.5	24.9	26.8	21.9
Avg or GM	overall				0.15	24%	24%	2.76	34.5	15.7	12.5	12.4

[1]Mean Hg concentrations (ug/g dry wt) and fluxes are reported as geometric means because results were log normally distributed.

[2] Presence (Y or N) of maximum concentrations and/or (unadjusted) fluxes subsurface. Percent showing subsurface maxima are shown in the last 4 lines of the table.

[3]FR = flux ratio = Recent flux / pre-industrial fluxes

[4]Recent and pre-industrial fluxes ($\mu g\ m^{-2}\ y^{-1}$) corrected for particle focusing. Averages on the last 4 lines are geometric means.

[5]Adjusted anthropogenic flux ($\mu g\ m^{-2}\ y^{-1}$) = $\Delta F_{adj,F}$ = [recent flux-pre-industrial flux-(pre-industrial flux*sedimentation ratio-pre-industrial flux)]/FF. Averages on the last 4 lines are geometric means.

[7]For Lake A only the ratios were calculated using concentrations at the surface (0-1 cm) and at a depth (10-20 cm)

Figure S1. Regression of soil ^{210}Pb fluxes vs latitude using all data points

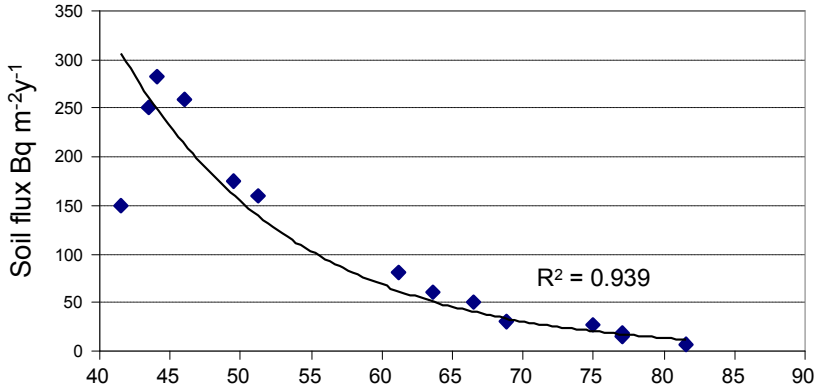

Figure S2. Excess ^{210}Pb versus accumulated dry weight for 48 lakes (in alphabetical order) and ^{137}Cs vs depth for Lake Hazen. ^{210}Pb profiles represent measured values as well as, for some cores, interpolated and extrapolated values for each core section. Trend line represents the log excess ^{210}Pb vs cumulative dry wt.

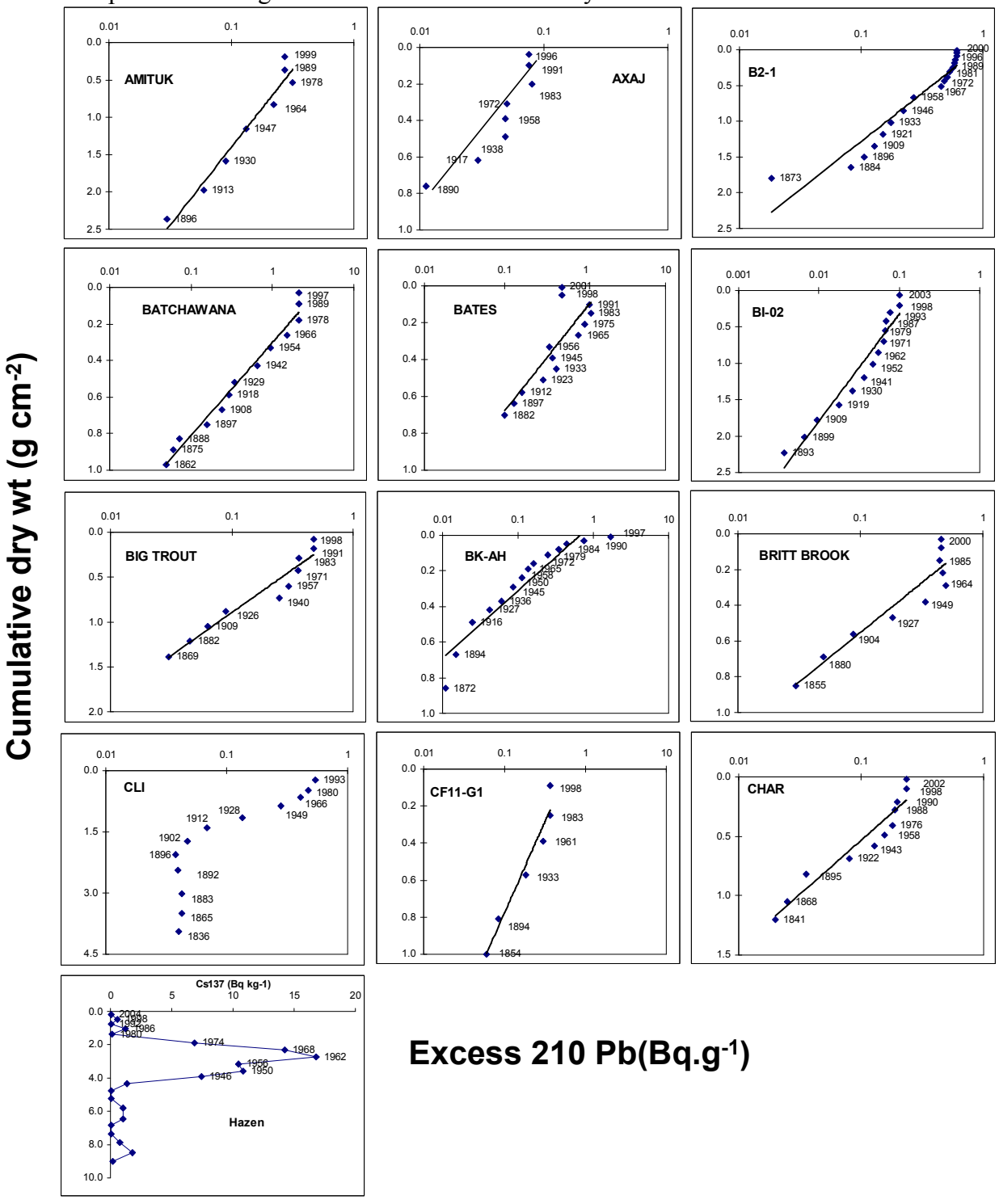

Figure S2. continued

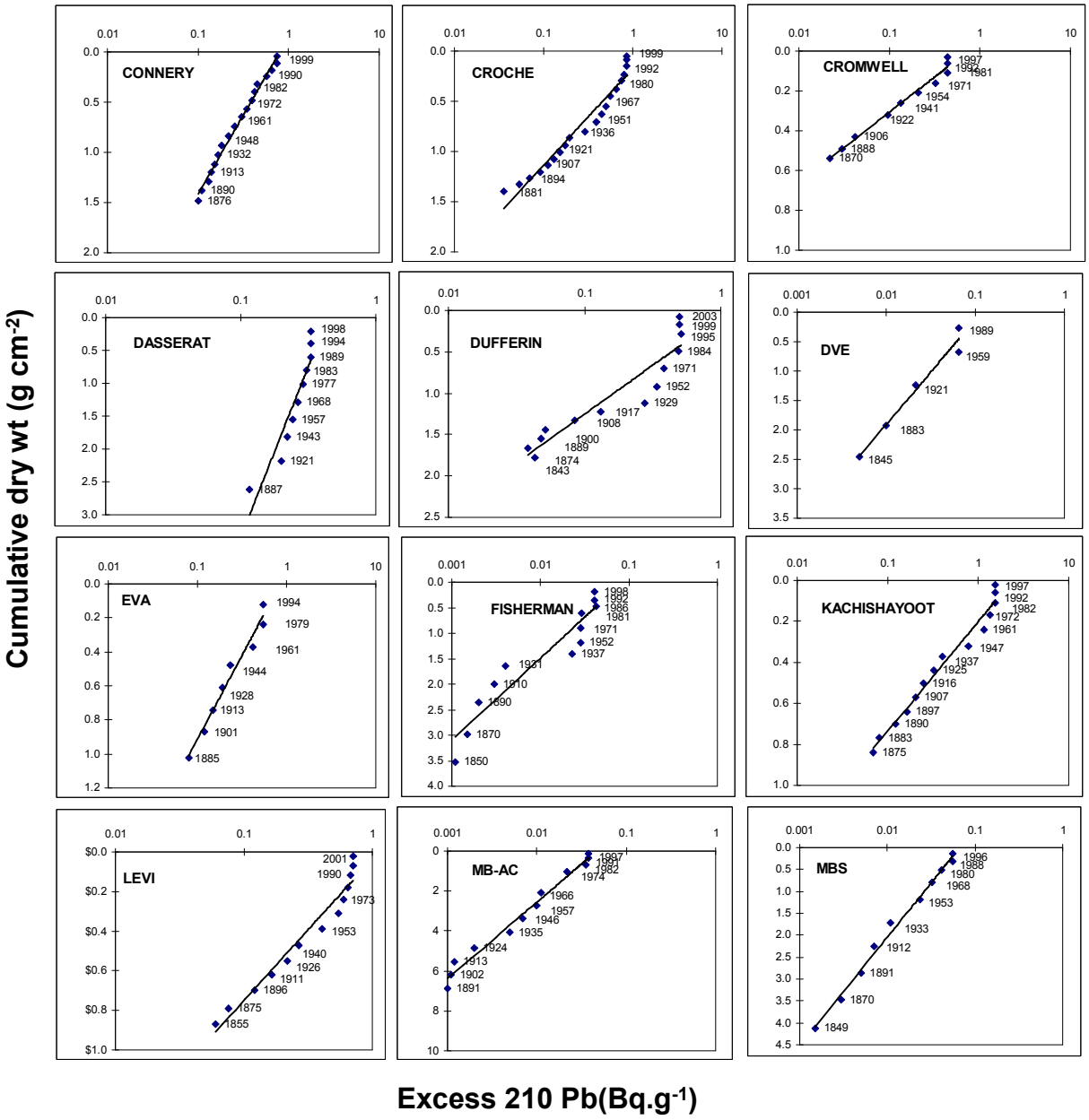

Figure S2. continued

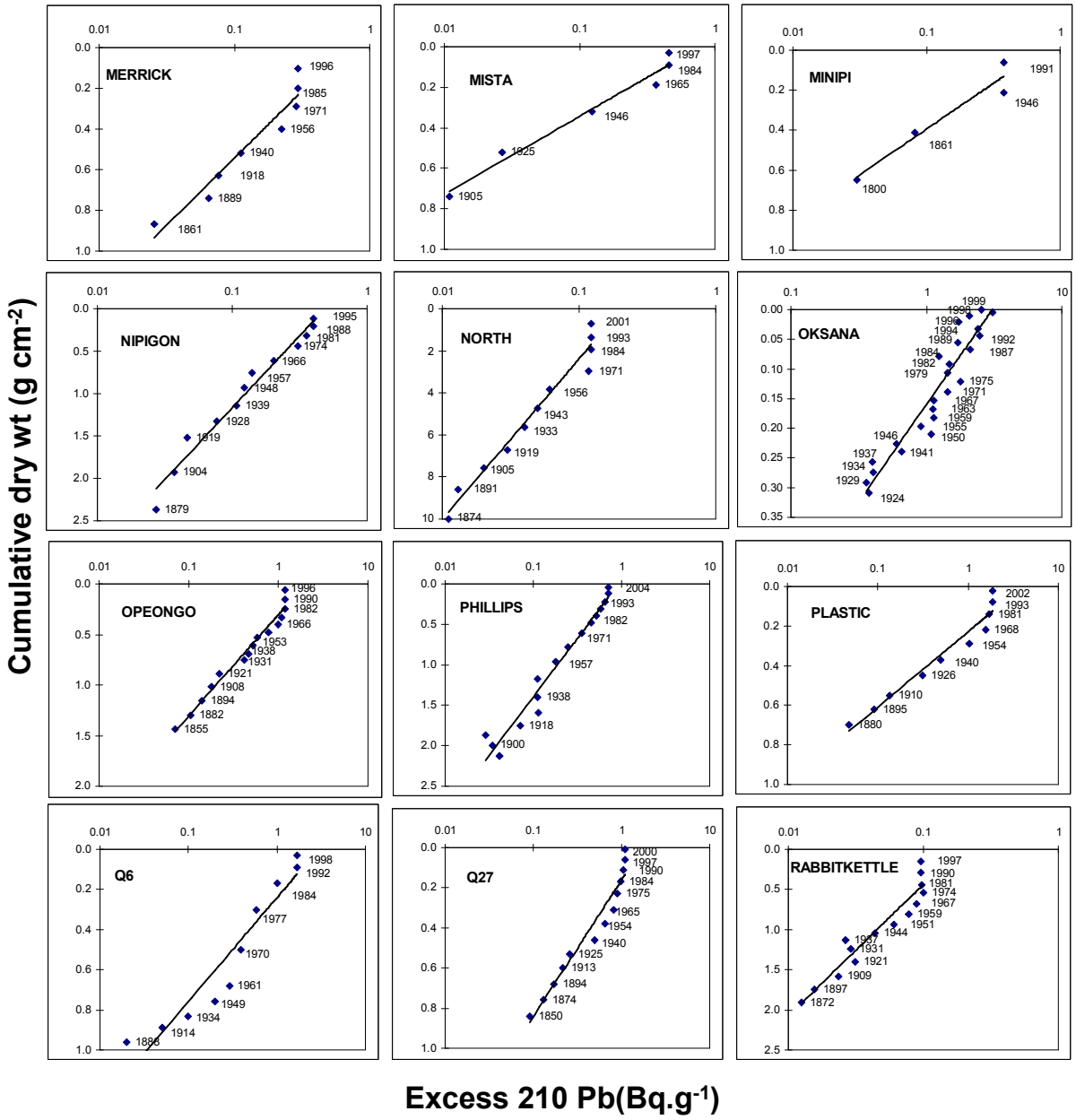

Figure S2 continued

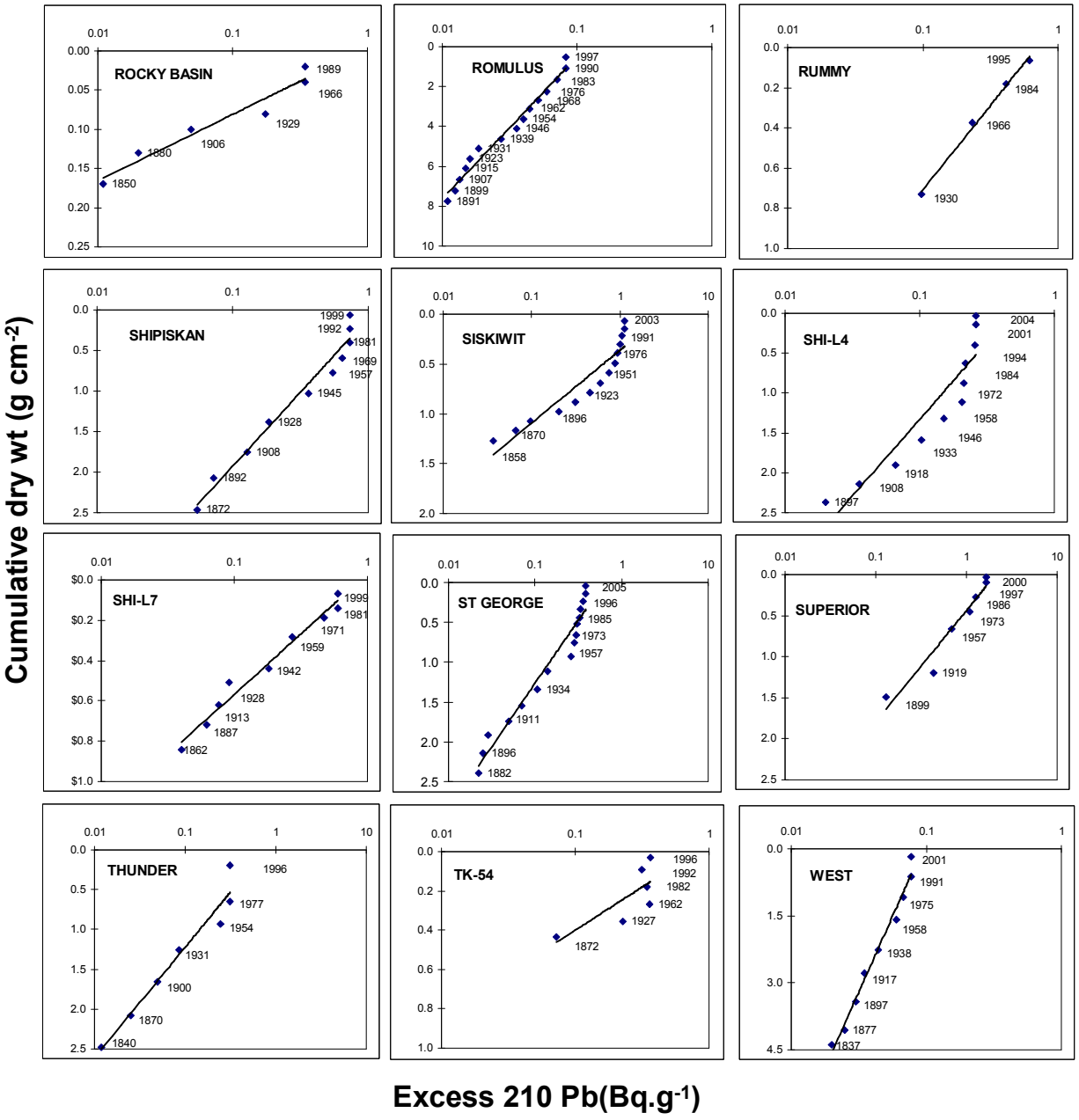

Figure S3. Relationship of pre-industrial and recent Hg fluxes (all unadjusted for sediment focusing and sedimentation) versus latitude in dated sediment cores from mid-latitude, subarctic and Arctic lakes. All statistics for flux vs latitude are based on log transformed flux data.

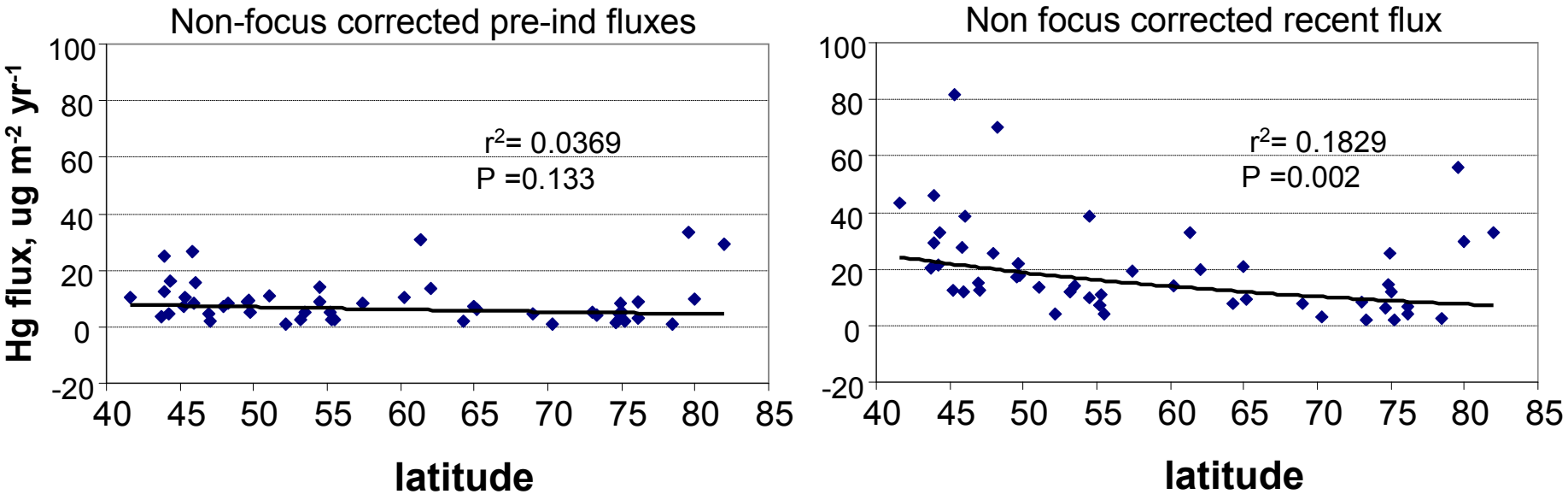

Figure S4. Relationship of recent (adjusted focusing and sedimentation) Hg fluxes to catchment area of mid-latitude lakes

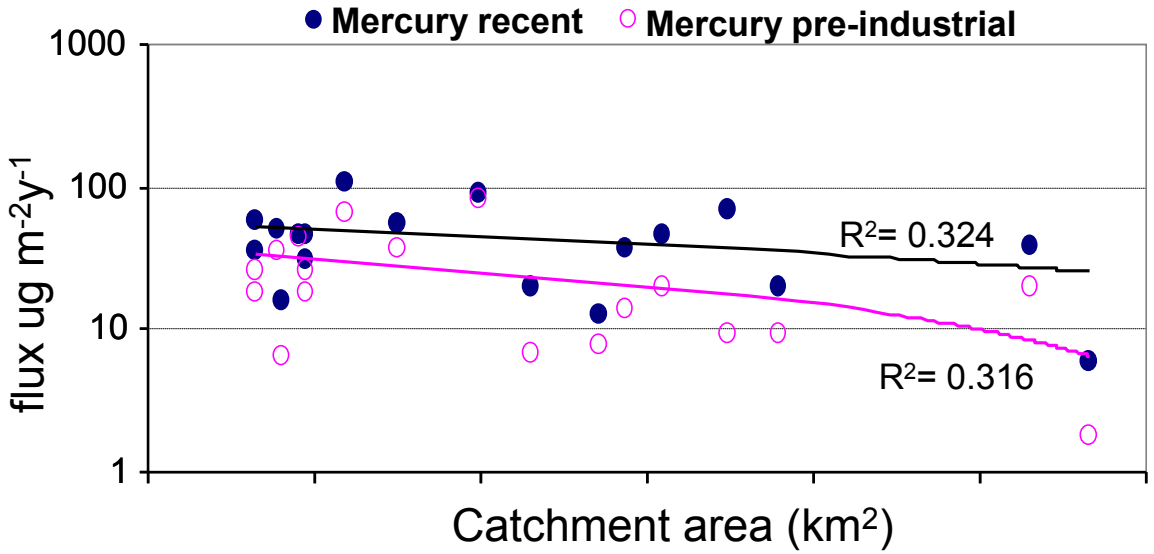

Figure S5. Mercury concentrations (ug/g dw) [squares] and (uncorrected) fluxes (µg m $^{-2}$y^{-1}) [circles] in dated 50 Arctic, subarctic and mid-latitude sediment cores. Horizonal axis represents median deposition year of each core section. Graphs are presented by region and lakes are sorted alphabetically. 1. Mercury: Arctic lakes.

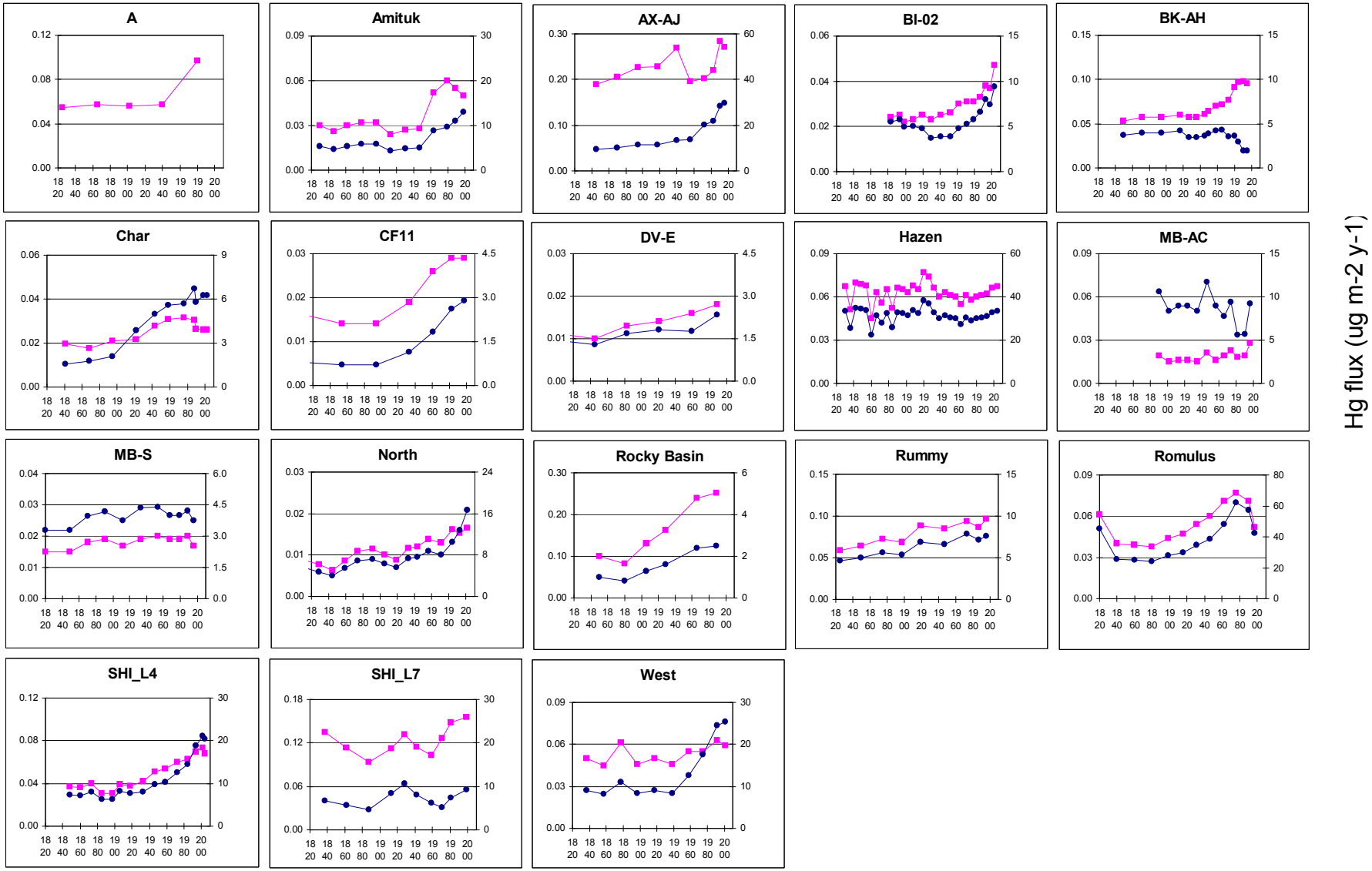

Figure S4. 2. Mercury: Subarctic lakes

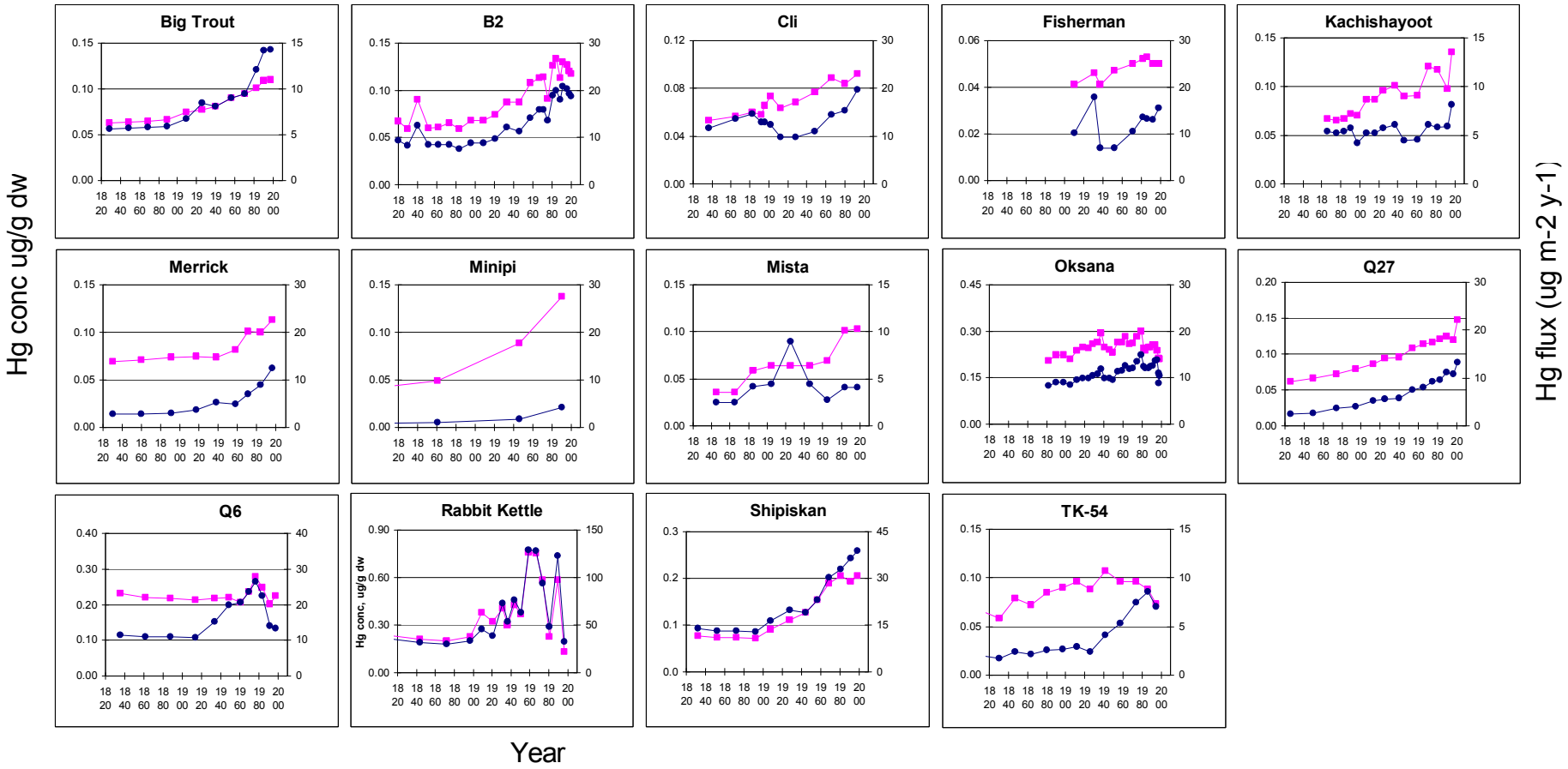

Figure S4. 3. Mercury: Mid-latitude lakes

Figure S6. Historical profiles of anthropogenic mercury deposition fluxes (µg m^{-2} y^{-1}; adjusted for sediment particle focusing and sedimentation rates) in Arctic, subarctic and mid-latitude sediment cores. Inset graphs for Arctic and subarctic cores show trends at a finer scale. All results for each sediment horizon represent dates estimated by the CRS model for the mid-point of each sample.

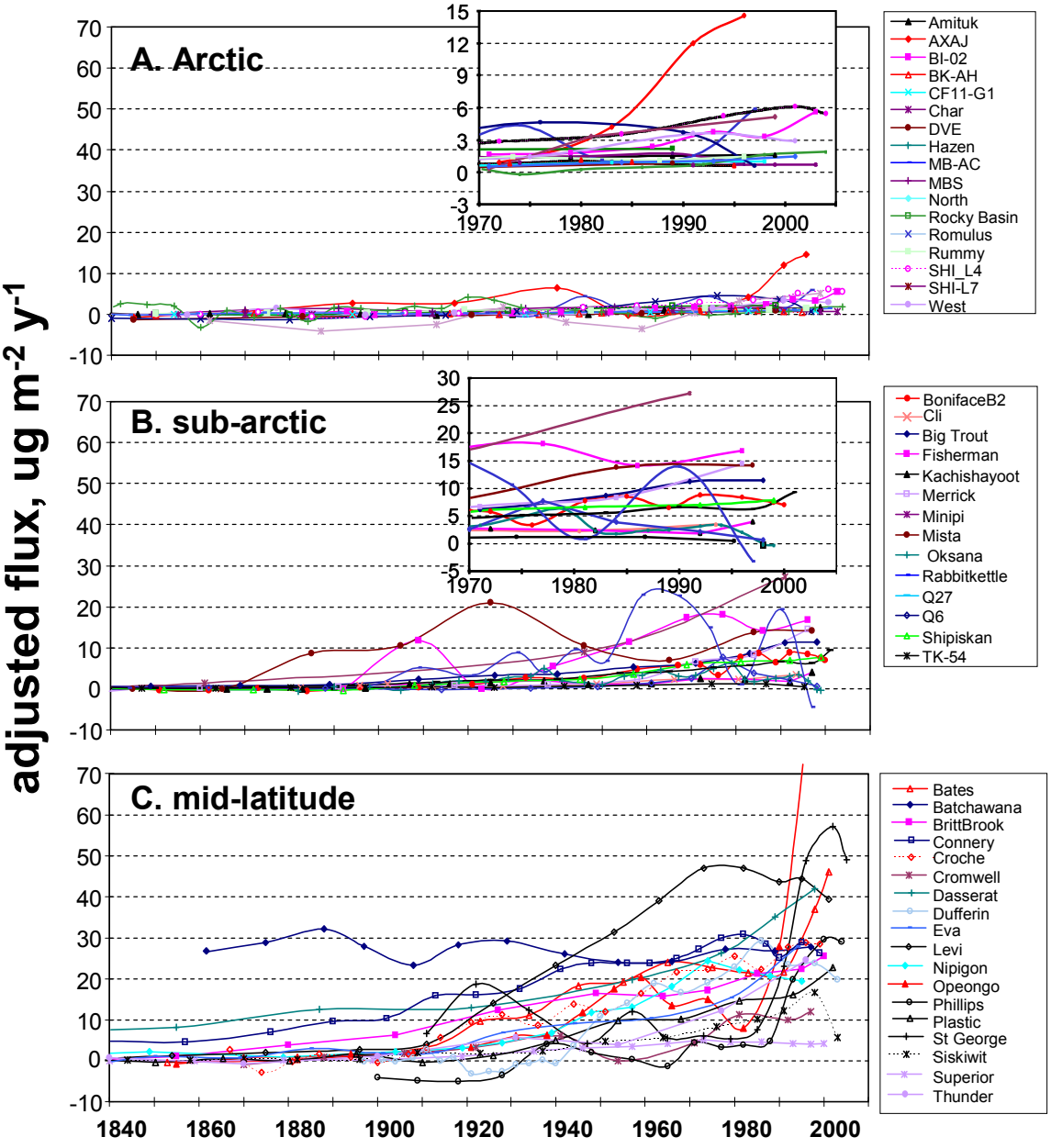

Figure S7. Plot of mercury FR vs the distance center (log or square root transformed) of the lake from the nearest ocean waters. For the regression of FR vs square root distance, Lake Hazen (80 km from the ocean) was omitted.

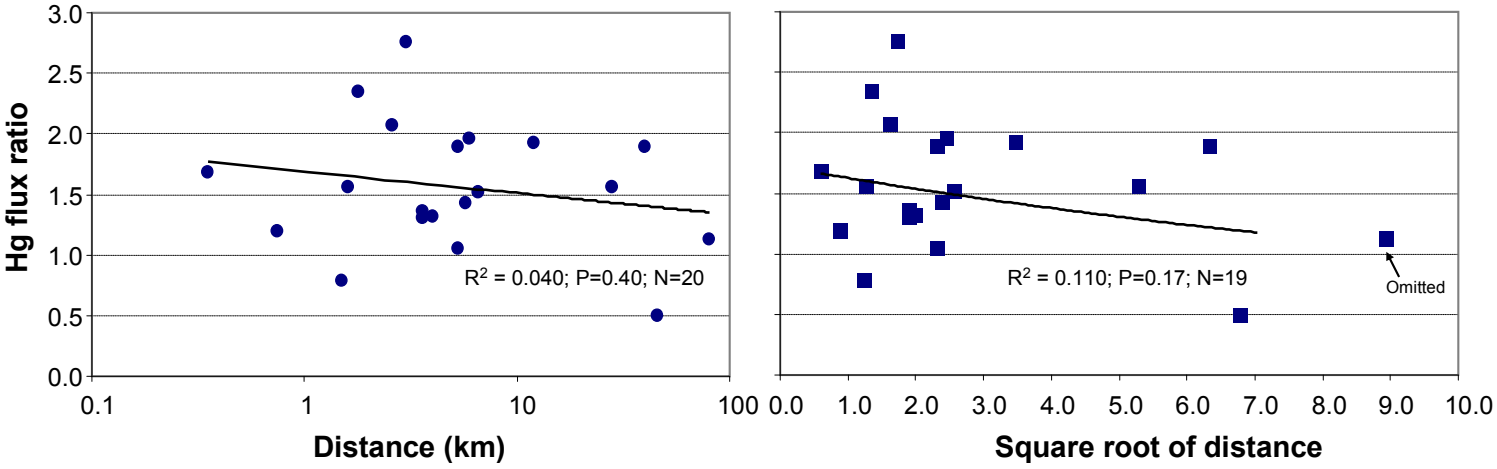

References

(1) EC and USEPA *State of the Great Lakes 2005*; Environment Canada and the US Environmental Protection Agency: Chicago, IL and Toronto ON, 2005; p 304 pp.

(2) Kajak, Z.; Kacprzak, K.; Polkowski, R., Chwytacz rurowy do pobierania prob dna. *Ekologia Polska Seria B* **1965,** *11*, 159-165.

(3) Brinkhurst, R. O.; Chua, K. E.; Batoosingh, E., Modifications in sampling procedures as applied to studies on the bacteria and tubificid oligochetes inhabiting aquatic sediments. *J. Fish. Res. Bd. Can.* **1969,** *26*, 2581-2593.

(4) Glew, J. R., A portable extruding device for close interval sectioning of unconsolidated core samples. *J. Paleolimnol.* **1988,** *1*, 235-239.

(5) Oldfield, F.; Appleby, P. G. Empirical testing of 210Pb dating models for lake sediments. In *Lake Sediments and Environmental History*, Haworth, E. Y.; Lund, J. W. G., Eds. University of Minnesota Press: Minneapolis, MN, 1984; pp 93-124.

(6) Eakins, J. D.; Morrison, R. T., A new procedure for determination of lead-210 in lake and marine sediments. *Int. J. Appl. Radiat. Isotope.* **1978,** *29*, 531-536.

(7) Preiss, N.; Méliées, M.-A.; Pourchet, M., A compilation of data on lead-210 concentration in surface air and fluxes at the air-surface water and water-sediment interfaces. *J. Geophys. Res.* **1996,** *1001*, 28847-28862.

(8) Wolfe, A. P.; Miller, G. H.; Olsen, C. A.; Forman, S. L.; Doran, P. T.; Holmgren, S. U. Geochronology of high latitude lake sediments. In *In: Developments in Paleoenvironmental Research, Vol. 8* Pienitz, R.; Douglas, M. S. V.; Smol, J. P., Eds. Springer: New York, NY, 2004.

(9) Hermanson, M. H., 210Pb and 137Cs chronology of sediments from small, shallow Arctic lakes. *Geochimica et Cosmochimica Acta* **1990,** *54*, 1443-1451.

(10) Muir, D. C. G.; Omelchenko, A.; Grift, N. P.; Savoie, D. A.; Lockhart, W. L.; Wilkinson, P.; Brunskill, G. J., Spatial Trends and Historical Deposition of Polychlorinated Biphenyls in Canadian Mid-latitude and Arctic Lake Sediments. *Environ. Sci. Technol.* **1996,** *30*, 3609-3617.

(11) Omelchenko, A.; Lockhart, W. L.; Wilkinson, P. *Study of the Depositional Characteristics of the Lake Sediments across Canada with Pb-210 and Cs-137*; Unpublished Internal Report, Freshwater Institute, Department of Fisheries and Oceans: Winnipeg, MB, Canada, 1995; p 48.

(12) Muir, D.; Halliwell, D.; Cheam, V. *Spatial Trends in Loadings and Historical Inputs of Mercury Inferred from Pan-Northern Lake Sediment Cores*; Northern Ecosystem Initiative NEI Secretariat, Environment Canada,: Yellowknife NT, 2003; p 17 pp.

(13) He, T.; Lu, J.; Yang, F.; Feng, X., Horizontal and vertical variability of mercury species in pore water and sediments in small lakes in Ontario. *Sci. Total Environ.* **2007,** *386*, 53-64.

(14) Jackson, T. A.; Muir, D. C. G.; Vincent, W. F., Historical variations in the stable isotope composition of mercury in Arctic lake sediments. *Environ Sci Technol* **2004,** *38*, 2813-21.

(15) Jackson, T. A.; Whittle, D. M.; Evans, M. S.; Muir, D. C. G., Evidence for mass-independent and mass-dependent fractionation of the stable isotopes of mercury by natural processes in aquatic ecosystems. *Applied Geochemistry* **2008,** *23*, 547-571.

(16) Lockhart, W. L.; Wilkinson, P.; Billeck, B. N.; Danell, R. A.; Hunt, R. V.; Brunskill, G. J.; Delaronde, J.; St Louis, V., Fluxes of mercury to lake sediments in central and northern Canada inferred from dated sediment cores. *Biogeochemistry* **1998,** *40*, 163-173.

(17) Mills, R. B.; Paterson, A. M.; Blais, J. M.; Lean, D. R. S.; Smol, J. P.; Mierle, G., Factors influencing the achievement of steady state in mercury contamination among lakes and catchments of south-central Ontario. *Can. J. Fish. Aquat. Sci.* **2009,** *66*, 187-200.
(18) Fitzgerald, W. F.; Engstrom, D. R.; Mason, R. P.; Nater, E. A., The case for atmospheric mercury contamination in remote areas. *Environmental Science and Technology* **1998,** *32*, 1-7.
(19) Outridge, P. M.; Stern, G. A.; Hamilton, P. B.; Percival, J. B.; McNeely, R.; Lockhart, W. L., Trace metal profiles in the varved sediment of an Arctic lake. *Geochim. Cosmochim. Acta* **2005,** *69*, 4881–4894.
(20) Christensen, J. H.; Brandt, J.; Frohn, L. M.; Skov, H., Modelling of mercury in the Arctic with the Danish Eulerian Hemispheric Model. *Atmos. Chem. Phys.* **2004,** *4*, 2251-2257.
(21) U.S. EPA *Mercury Study Report to Congress; EPA-452-97-003-010. Volume III: Fate and Transport of Mercury in the Environment*; United States Environmental Protection Agency, Office of Air and Radiation: Washington, DC, 1997.
(22) Gbor, P. K.; Wen, D.; Meng, F.; Yang, F.; Sloan, J. J., Modeling of mercury emission, transport and deposition in North America. *Atmos. Environ.* **2007,** *41*, 1135-1149.
(23) Dastoor, A. P.; Larocque, Y., Global circulation of atmospheric mercury: A modelling study. *Atmos. Environ.* **2004,** *38*, 147-161.
(24) Dastoor, A. P.; Davignon, D.; Theys, N.; Van Roozendael, M.; Steffen, A.; Ariya, P. A., Modeling dynamic exchange of gaseous elemental mercury at polar sunrise. *Environ. Sci. Technol.* **2008,** *42*, 5183-5188.
(25) Constant, P.; Poissant, L.; Villemur, R.; Yumvihoze, E.; Lean, D., Fate of inorganic mercury and methyl mercury within the snow cover in the low arctic tundra on the shore of Hudson Bay (Québec, Canada). *J. Geophys. Res. D: Atmos.* **2007,** *112*.
(26) Garbarino, J. R.; Snyder-Conn, E.; Leiker, T. J.; Hoffman, G. L., Contaminants in arctic snow collected over northwest Alaskan sea ice. *Water Air Soil Poll.* **2002,** *139*, 183-214.
(27) Berg, T.; Aspmo, K.; Steinnes, E., Transport of Hg from Atmospheric mercury depletion events to the mainland of Norway and its possible influence on Hg deposition. *Geophys. Res. Let.* **2008,** *35*.
(28) Miller, E. K.; Vanarsdale, A.; Keeler, G. J.; Chalmers, A.; Poissant, L.; Kamman, N. C.; Brulotte, R., Estimation and mapping of wet and dry mercury deposition across northeastern North America. *Ecotoxicology* **2005,** *14*, 53-70.
(29) Perry, E.; Norton, S. A.; Kamman, N. C.; Lorey, P. M.; Driscoll, C. T., Deconstruction of historic mercury accumulation in lake sediments, northeastern United States. *Ecotoxicology* **2005,** *14*, 85-99.
(30) Fitzgerald, W. F.; Engstrom, D. R.; Lamborg, C. H.; Tseng, C.-M.; Balcom, P. H.; Hammerschmidt, C. R., Modern and historic atmospheric mercury fluxes in northern Alaska: Global sources and Arctic depletion. *Environ. Sci. Technol.* **2005,** *39*, 557-568.
(31) Nozaki, Y.; DeMaster, D. J.; Lewis, D. M.; Turekian, K. K., Atmospheric 210Pb fluxes determined from soil profiles. *J. Geophs. Res.* **1978,** *83*, 4047-4051.
(32) Davis, R. B.; Hess, C. T.; Norton, S. A.; Hanson, D. W.; Hoagland, K. D.; Anderson, D. S., 137Cs and 210Pb dating of sediments from soft-water lakes in New England (U.S.A.) and Scandinavia, a failure of 137Cs dating. *Chemical Geology* **1984,** *44*, 151-185.
(33) Eisenreich, S. J.; Capel, P. D.; Robbins, J. A.; Bourbonniere, R., Accumulation and diagenesis of chlorinated hydrocarbons in lacustrine sediments. *Environ. Sci. Technol.* **1989,** *23*, 1116-1126.

(34) Talbot, R. W.; Andren, A. W., Relationships between Pb and 210Pb in aerosol and precipitation at a semiremote site in northern Wisconsin. *J. Geophys. Res.* **1983,** *88*, 6752-6760.
(35) Turekian, K. K.; Nozaki, Y.; Benninger, L. K., Geochemistry of atmospheric radon and radon products. *Ann. Rev. Earth Plant. Sci.* **1977,** *5*, 227-255.